Journal of Intelligent & Robotic Systems
https://doi.org/10.1007/s10846-020-01260-7

Model Reference Adaptive Control of Switched Dynamical Systems with Applications to Aerial Robotics

Robert B. Anderson[1] · Julius A. Marshall[1] · Andrea L'Afflitto[1] · James M. Dotterweich[2]

Received: 1 January 2020 / Accepted: 4 September 2020

Abstract

This paper presents an adaptive control law for unknown nonlinear switched plants that must follow the trajectory of user-defined linear switched reference models. The effectiveness of the proposed control architecture is proven in two alternative frameworks, that is, analyzing Carathéodory and Filippov solutions of discontinuous differential equations. Numerical and experimental data verify the applicability of the theoretical results to problems of practical interest. The proposed numerical simulation involves the design of a model reference adaptive control law to regulate the roll dynamics of a reconfigurable delta-wing aircraft. The proposed flight tests involve an aerial robot tasked with autonomously mounting a camera of unknown inertial properties to a vertical surface.

Keywords Model reference adaptive control · Switched dynamical systems · Carathéodory solutions · Filippov solutions · Aerial robots

1 Introduction

The dynamics of numerous mechanical and electronic systems are subject to instantaneous changes and are best captured by switched dynamical systems, that is, differential equations with discontinuous right-hand sides. Examples of switched dynamical models involve mechanical systems subject to velocity jumps and force discontinuities [6, 45]. Furthermore, the closed-loop dynamics of systems regulated by discontinuous control algorithms such as time-optimal control laws [7, pp. 110-117], variable structure control laws [27, pp. 552-579], [14, 34, 52], and supervisory control architectures [29, 41, 42, 54] may be captured by switched models. Substantial complexity in the analysis and control synthesis of discontinuous dynamical systems is given by the fact that their solutions may not exist or may not be unique [27, Ch. 3]. Furthermore, the notion of solution of a switched differential equation is not univocal. Indeed, Carathéodory [8], Filippov [16], Krasovskii [30], and Euler [12] solutions, to name a few, have been introduced to better capture the behavior of different classes of discontinuous dynamical systems; for additional details, see [13, 20, 23, 49] and the references therein.

In this paper, we design an adaptive control law for unknown nonlinear switched plants so that their trajectories track the trajectories of user-defined switched reference models. The mapping between the switching signal and the plant dynamics is considered as unknown. The switching signal is assumed to be a known function of time since in model reference adaptive control, the reference model is user-defined and independent of the plant state.

The effectiveness of the proposed model reference adaptive control law is proven in two alternative frameworks, that is, by considering Carathéodory and Filippov solutions of discontinuous differential equations. These two frameworks

This work was supported in part by the US Army Research Lab (ARL), DARPA, and ONR under Grants no. 40304747, D18AP00069, and N000141912422, respectively.

✉ Andrea L'Afflitto
a.lafflitto@vt.edu

Robert B. Anderson
andersonb@vt.edu

Julius A. Marshall
mjulius@vt.edu

James M. Dotterweich
james.m.dotterweich.civ@mail.mil

[1] Grado Department of Industrial and Systems Engineering, Virginia Tech, Blacksburg, VA 24061, USA

[2] CCDC Army Research Laboratory, Aberdeen Proving Ground, Adelphi, MD 21005, USA

Published online: 23 September 2020

have been chosen since both Carathéodory and Filippov solutions of discontinuous dynamical systems are usually more suitable to analyze the dynamics of mechanical systems. Indeed, both Carathéodory and Filippov solutions are absolutely continuous and hence, have bounded variations over bounded time intervals, and their time derivatives exist almost everywhere [50, pp. 127-130]. Applying the Carathéodory framework, we prove that if the switching signal is characterized by an arbitrarily small, but non-zero, dwell-time, then solutions of both the trajectory tracking error's and the adaptive gains' dynamics exist, are unique, and are defined almost everywhere over the semi-infinite time horizon, and the plant trajectory asymptotically converges to the reference model's trajectory. Employing the Filippov framework, we prove that if the switching signal is Lebesgue integrable and has countably many points of discontinuity, then maximal solutions of both the trajectory tracking error and the adaptive gains dynamics exist and are defined almost everywhere on the semi-infinite time horizon, and the trajectory tracking error converges to zero asymptotically. Considering Filippov solutions, the switching signal may have zero dwell-time, but the uniqueness of the solutions of the trajectory tracking error's and the adaptive gains' dynamics cannot be proven.

The theoretical framework employed in this paper does not allow to control plants whose dimensions vary as arbitrary functions of time. However, the proposed framework allows to address those problems, wherein the plant's dynamics is in partial-state equilibrium [19, Def. 4.1] for some values of the switching signal. In these cases, the dynamics of those components of the state vector that are at equilibrium can be disregarded, and only the dynamics of those components of the state vector that are not at equilibrium is regulated by applying the proposed framework.

To the authors' best knowledge, this is the first paper to deduce model reference adaptive control laws for unknown nonlinear switched plants and switched reference models employing the Carathéodory and the Filippov frameworks. Furthermore, the proposed model reference adaptive control laws are unique for their ability to regulate unknown nonlinear plants without any restrictions on the dwell-time. The design of model reference controls for linear switched systems was addressed in [55, 57]. The authors in [61] proposed an H_∞-based adaptive control law for switched linear dynamical systems. Supervisory control architectures involving multiple adaptive control laws have been proposed in [22, 28, 39, 40, 43, 51, 58, 59] to regulate linear uncertain dynamical systems, while guaranteeing user-defined levels of performance in the transient regime. In [17, 26, 44], the authors devised an adaptive sliding mode control law for switched dynamical systems that are linear in the parameters and subject to external disturbances, and proved the validity of their results in the Filippov and the Krasovskii frameworks. The design of model reference adaptive control laws for uncertain nonlinear plants was presented in [60] employing the average dwell-time method under asynchronous switching, and [56] analyzing classical solutions of the closed-loop system. An adaptive controller for nonlinear systems, which does not rely on any restrictions on the dwell-time, has been presented in [35]. However, this result is achieved by assuming that the linear portion of the plant dynamics is the same for all switched systems. An adaptive control law for nonlinear switched systems with arbitrary switching is presented in [10]. However, these results apply if there exists a diffeomorphism such that the plant dynamics is equivalent to a cascaded dynamical system.

The effectiveness of the proposed results is firstly verified numerically. Specifically, we present a numerical example that involves the design of a control law for the roll dynamics of a delta-wing aircraft that can switch between two alternative configurations, namely a stable and less responsive configuration and an unstable and more responsive configuration. Reconfigurable aircraft are particularly advantageous for those applications, wherein the vehicle must operate in multiple flight regimes by rapidly changing its geometric and aerodynamic properties [4, 21, 46, 48, 53]. However, rapid or instantaneous changes in the aircraft configuration or the reference model underlying the control architecture may induce instabilities. The robustness of the proposed model reference adaptive control law is challenged by assuming that the aircraft aerodynamic coefficients are unknown in all configurations and by switching arbitrarily fast both the plant's and the reference model's dynamics. Control algorithms for morphing-wing aircraft have been investigated in [9] using an H_∞ control framework, [18] employing a backstepping approach, and [25] using a variable structure switched control law. Furthermore, a supervisory control architecture has been presented in [25] to regulate a vertical take-off and landing aircraft modeled as switched dynamical systems. None of the control techniques for uncertain, switched, nonlinear plants that we surveyed is suitable to regulate plants in the same form as the dynamical model in the proposed numerical example. Thus, the performance of the proposed model reference adaptive control law is compared to the performance of the classical model reference adaptive control law [33, Ch. 9] obtained considering only one of the two aircraft configurations. In particular, it is shown how, considering only the dynamical model for the less responsive configuration, the classical model reference adaptive control law is unable to regulate the plant dynamics, and the trajectory tracking error diverges. Alternatively, considering only the dynamical model for the more responsive configuration, the trajectory tracking

error, the control effort, and the computational time are considerably larger than the trajectory tracking error, the control effort, and the computational time achieved by applying the proposed adaptive law.

The effectiveness of the proposed results is verified also by means of flight tests. These flight tests involve an autonomous aerial robot, that is, a tilt-rotor quadcopter equipped with a robotic arm, whose task is to install a camera of unknown mass on a vertical surface. The aerial robot holds the camera by means of a suction cup, and linear strip fasteners are used to attach the camera to the vertical surface. A switched dynamical model is employed to capture the aerial robot's dynamics. Indeed, as soon as the robotic arm impacts the vertical surface, the vehicle's forward motion is impeded by reaction forces. Furthermore, while the camera is being installed on the vertical surface, the aerial robot's yaw and roll dynamics and lateral motion are constrained by the suction cup and the linear fabric strip fasteners.

Flight tests results clearly show that the proposed model reference adaptive control law guarantees successful completion of the assigned task despite uncertainties on the aerial manipulator's dynamics. The problem of designing control algorithms for aerial systems interacting with hard surfaces, such as walls and floors, has been investigated recently by applying feedback-linearizing control laws within a hybrid systems framework [1, 37, 38]. It is worthwhile to remark that, imposing some conditions on the minimum dwell-time, the results in [1, 37, 38] allow instantaneous increases of the trajectory tracking error at switching times, whereas the proposed adaptive control framework does not restrict the plant's minimum dwell time and does not allow instantaneous variations in the trajectory tracking error. To the authors' best knowledge, this is the first paper to verify experimentally a switched adaptive control framework within the context of aerial robotics.

2 Mathematical Preliminaries

2.1 Notation

In this section, we establish some of the notation used in this paper. Let $\mathbb{N}$ denote the *set of positive integers*,$\mathbb{R}$ denote the *set of real numbers*, $\mathbb{C}$ the *set of complex numbers*, $\mathbb{R}^n$ the *set of* $n \times 1$ *real column vectors*, $\mathbb{R}^{n\times m}$ the *set of* $n \times m$ *real matrices*, $\mathcal{B}_\varepsilon(x)$ the *open ball centered* at $x \in \mathbb{R}^n$ with *radius* $\varepsilon > 0$, and $\partial\mathcal{B}_\varepsilon(x)$ the *sphere centered* at $x \in \mathbb{R}^n$ with *radius* ε.

The *indicator function* of the set $\mathcal{A} \subset \mathbb{R}^n$ is denoted by $\mathbf{1}_\mathcal{A} : \mathcal{A} \to \{0, 1\}$ and is defined so that if $x \in \mathcal{A}$, then $\mathbf{1}_\mathcal{A}(x) = 1$, and if $x \notin \mathcal{A}$, then $\mathbf{1}_\mathcal{A}(x) = 0$. The *Lebesgue measure* of a set $\mathcal{S} \subset \mathbb{R}^{n\times m}$ is denoted by $\mu(\mathcal{S})$, and integrals are in the sense of Lebesgue. A property $\mathfrak{P}$ is verified *almost everywhere* with respect to the Lebesgue measure $\mu(\cdot)$ on a set $\mathcal{X} \subseteq \mathbb{R}^n$ if there exists $\mathcal{N} \subset \mathcal{X}$ such that $\mu(\mathcal{N}) = 0$ and $\mathfrak{P}$ is verified by all $x \in \mathcal{X} \setminus \mathcal{N}$. In this case, we write $\mathfrak{P}$ is verified for $x \in \mathcal{X}$ a.e.

The ith *vector of the canonical basis of* $\mathbb{R}^n$ is denoted by $\mathbf{e}_{i,n}$. The *zero vector* in $\mathbb{R}^n$ is denoted by 0_n or 0, the *zero* $n \times m$ *matrix* in $\mathbb{R}^{n\times m}$ is denoted by $0_{n\times m}$ or 0, and the *identity matrix* in $\mathbb{R}^{n\times n}$ is denoted by I_n or I. The diagonal matrix, whose diagonal entries are given by the components of $z \in \mathbb{R}^n$, is denoted by $\mathrm{diag}(z)$. The *transpose of* $B \in \mathbb{R}^{n\times m}$ is denoted by B^T, the *rank of* B is denoted by $\mathrm{rank}(B)$, and the *trace of* $A \in \mathbb{R}^{n\times n}$ is denoted by $\mathrm{tr}(A)$. The *spectrum* of $A \in \mathbb{R}^{n\times n}$ is denoted by $\mathrm{spec}(A)$, and the eigenvalues of A with minimum real part are denoted by $\lambda_{\min}(A)$. We write $\|\cdot\|$ for the *Euclidean vector norm* and the corresponding *equi-induced matrix norm*. Furthermore, we write $\|\cdot\|_\mathrm{F}$ for the *Frobenius matrix norm*. The *Kronecker product of* $A \in \mathbb{R}^{n\times m}$ *and* $B \in \mathbb{R}^{l\times p}$ is denoted by $A \otimes B$.

2.2 Fundamentals of Switched Dynamical Systems – Carathéodory Framework

In the following, we recall fundamental properties of the nonlinear dynamical system with time-dependent switching

$$\dot{x}(t) = f_{\sigma(t)}(t, x(t)), \qquad x(t_0) = x_0, \qquad t \geq t_0, \tag{1}$$

where $f_s : [t_0, \infty) \times \mathcal{D} \to \mathbb{R}^n$, $s \in \Sigma$, $\Sigma \subset \mathbb{N}$ is bounded and denotes the *set of switching indexes*, the set $\mathcal{D} \subseteq \mathbb{R}^n$ is open, connected, and such that $0 \in \mathcal{D}$, the *switching signal* $\sigma : [t_0, \infty) \to \Sigma$ is piece-wise constant, $\sigma(t) = \lim_{\tau\to t^+} \sigma(\tau)$ for each $t \geq t_0$, the *sth dynamical model* $f_s(\cdot, x)$ is piece-wise continuous in t for all $(s, x) \in \Sigma \times \mathcal{D}$, $f_s(t, 0) = 0$ for all $(s, t) \in \Sigma \times [t_0, \infty)$, and $f_s(t, \cdot)$ is Lipschitz continuous in x uniformly in t for all t in compact subsets of $[t_0, \infty)$ and for all $s \in \Sigma$; we recall that $\sigma(\cdot)$ is piece-wise constant if and only if $\sigma(\cdot)$ has a finite number of points of discontinuity on any compact subset of $[t_0, \infty)$ and is constant between two consecutive points of discontinuity. In this paper, we define *switching times* as the points of discontinuity of $\sigma(\cdot)$.

Definition 1 ([36, p. 10]) A function $x : [t_0, \infty) \to \mathcal{D}$ is a *Carathéodory solution of* Eq. 1 if

$$x(t) = x_0 + \int_{t_0}^{t} f_{\sigma(\tau)}(\tau, x(\tau))\mathrm{d}\tau \quad t \geq t_0 \ \text{ a.e.} \tag{2}$$

It is worthwhile to recall that if $x(\cdot)$ verifies (2), then $x(\cdot)$ is absolutely continuous [50, p. 128]. Furthermore, Lipschitz continuity of $f_s(t, \cdot)$ for all t in compact subsets of $[t_0, \infty)$ and for all $s \in \Sigma$ is sufficient to guarantee the existence of a unique solution of Eq. 1 in the

sense of Carathéodory [16, Th. 1.2]. Next, we recall the notion of uniform boundedness of Carathéodory solutions of nonlinear dynamical systems under time-dependent switching.

Definition 2 The switched dynamical system (1) is *bounded uniformly in both* $t_0 \in [0, \infty)$ *and* $\sigma(\cdot)$ if there exists $\gamma > 0$, which is independent of both $t_0 \in [0, \infty)$ and $\sigma(\cdot)$, such that for every $\delta \in (0, \gamma)$, there exists $\varepsilon(\delta) > 0$ such that $x_0 \in \mathcal{B}_\delta(0) \cap \mathcal{D}$ implies that $\|x(t)\| < \varepsilon, t \geq t_0$ a.e. The switched dynamical system (1) is *globally bounded uniformly in both* $t_0 \in [0, \infty)$ *and* $\sigma(\cdot)$ if $\mathcal{D} = \mathbb{R}^n$ and for every $\delta > 0$ there exists $\varepsilon(\delta) > 0$ such that $x_0 \in \mathcal{B}_\delta(0)$ implies that $\|x(t)\| < \varepsilon, t \geq t_0$ a.e.

2.3 Fundamentals of switched dynamical systems – Filippov framework

In the following, we recall fundamental notions concerning Filippov solutions of the nonlinear dynamical system with time-dependent switching (1), where the sth dynamical model $f_s(\cdot, x)$, $s \in \Sigma$, is Lebesgue integrable and essentially locally bounded uniformly in $t \in [t_0, \infty)$ for all $(s, x) \in \Sigma \times \mathcal{D}$, $f_s(t, 0) = 0$ for all $(s, t) \in \Sigma \times [t_0, \infty)$, and $f_s(t, \cdot)$ is continuous in x uniformly in t for all t in compact subsets of $[t_0, \infty)$ and for all $s \in \Sigma$, $\mathcal{D} \subseteq \mathbb{R}^n$ is open, connected, convex, and such that $0 \in \mathcal{D}$, the set of switching indexes $\Sigma \subset \mathbb{N}$ is bounded, and the switching signal $\sigma : [t_0, \infty) \to \Sigma$ is Lebesgue integrable and has countably many discontinuities. It is worthwhile to note that, while employing the Filippov framework, we do not assume that $\sigma(\cdot)$ has a finite number of switching times on compact subsets of $[t_0, \infty)$.

Definition 3 ([16, p. 85]) Let $\mathcal{I} \subseteq [t_0, \infty)$ be connected and such that $t_0 \in \mathcal{I}$. If $x : \mathcal{I} \to \mathcal{D}$ is absolutely continuous and such that

$$\dot{x}(t) \in K[f_{\sigma(t)}](t, x(t)), \qquad t \in \mathcal{I} \ \text{ a.e.}, \tag{3}$$

where

$$K[f_s](t, x) \triangleq \bigcap_{\delta > 0} \bigcap_{\mu(\mathcal{N})=0} \overline{\text{co}}\left(f_s\left(t, \mathcal{B}_\delta(x) \setminus \mathcal{N}\right)\right), \quad (s, t, x) \in \Sigma \times [t_0, \infty) \times \mathcal{D}, \tag{4}$$

denotes the *Filippov regularization of* Eq. 1, $\bigcap_{\mu(\mathcal{N})=0}$ denotes the intersection over sets $\mathcal{N}$ of measure zero, and $\overline{\text{co}}(\cdot)$ denotes the convex closure of its argument, then $x(\cdot)$ is a *Filippov solution of* Eq. 1. If there do not exist a connected set $\overline{\mathcal{I}} \subseteq [t_0, \infty)$ and a Filippov solution $\overline{x} : \overline{\mathcal{I}} \to \mathcal{D}$ of Eq. 1 such that $\mathcal{I} \subset \overline{\mathcal{I}}$ and $\overline{x}(t) = x(t), t \in \mathcal{I}$ a.e., then $x : \mathcal{I} \to \mathcal{D}$ is a *maximal Filippov solution* of Eq. 1.

It follows from Theorem 2.7 of [16], the boundedness of Σ, the integrability and the essential local boundedness of $f_s(\cdot, x)$, $s \in \Sigma$, uniformly in $t \in [t_0, \infty)$ for all $(s, x) \in \Sigma \times \mathcal{D}$, and the continuity of $f_s(t, \cdot)$ in x uniformly in t for all t in compact subsets of $[t_0, \infty)$ and for all $s \in \Sigma$, that there exists a solution of Eq. 1 in the sense of Filippov. Next, we recall the notions of directional derivatives, generalized directional derivatives, and regular functions. For the statement of these definitions, let $[z, z + a) \triangleq \{z + \theta a, \theta \in [0, 1)\}$, $(z, a) \in \mathbb{R}^l \times \mathbb{R}^l$, denote a *line segment in* $\mathbb{R}^l$ and let

$$\text{vcone}(\mathcal{Q}, z) \triangleq \left\{\xi \in \mathbb{R}^l : \exists \alpha > 0 \text{ such that } [z, z + \alpha\xi) \subset \mathcal{Q}\right\} \tag{5}$$

denote the *variational cone* of $\mathcal{Q} \subseteq \mathbb{R}^l$ at z.

Definition 4 [5, pp. 63-64],[11, p. 39] Let $W : \mathcal{Q} \to \mathbb{R}$ be Lipschitz continuous, where $\mathcal{Q} \subseteq \mathbb{R}^l$. The *right directional derivative of* $W(\cdot)$ *at* $z \in \mathcal{Q}$ *along the direction of* $q \in \text{vcone}(\mathcal{Q}, z)$ is defined as

$$W'(z, q) \triangleq \lim_{\tau \to 0^+} \frac{W(z + \tau q) - W(z)}{\tau}, \quad (z, q) \in \mathcal{Q} \times \text{vcone}(\mathcal{Q}, z). \tag{6}$$

The *generalized directional derivatives of* $W(\cdot)$ *at* $z \in \mathcal{Q}$ *along the direction of* $q \in \text{vcone}(\mathcal{Q}, z)$ is defined as

$$W^0(z, q) \triangleq \limsup_{\substack{y \to z \\ \tau \to 0^+}} \frac{W(y + \tau q) - W(y)}{\tau}, \quad (z, q) \in \mathcal{Q} \times \text{vcone}(\mathcal{Q}, z). \tag{7}$$

If $W'(z, q) = W^0(z, q)$ for all $q \in \text{vcone}(\mathcal{Q}, z)$, then $W(\cdot)$ is *regular at* $z \in \mathcal{Q}$.

Next, we recall the notion of Clarke gradient. This definition is essential to state a generalization of the LaSalle-Yoshizawa theorem for Lebesgue measurable dynamical models.

Definition 5 [11, p. 10] Let $W : \mathcal{Q} \to \mathbb{R}$, where $\mathcal{Q} \subseteq \mathbb{R}^l$. The *Clarke gradient* of $W(\cdot)$ at $z \in \mathcal{Q}$ is defined as

$$\partial W(z) \triangleq \left\{p \in \mathbb{R}^l : W^0(z, q) \leq p^{\mathrm{T}} q, \forall q \in \text{vcone}(\mathcal{Q}, z)\right\}, \quad z \in \mathcal{Q}, \tag{8}$$

where $W^0(\cdot, \cdot)$ denotes the generalized directional derivatives of $W(\cdot)$.

In the following, we provide an expression of the Clarke gradient for Lipschitz continuous functions. For the statement of this result, recall that, by Rademacher's theorem [15, Th. 3.1.6], if $V : [t_0, \infty) \times \mathcal{D} \to \mathbb{R}$ is Lipschitz

continuous, then $V(\cdot,\cdot)$ is differentiable almost everywhere, and define

$$\Omega_V \triangleq \left\{(t,x) \in [t_0,\infty) \times \mathcal{D} : \left[\frac{\partial V(t,x)}{\partial t}, \frac{\partial V(t,x)}{\partial x}\right]^{\mathrm{T}} \text{ is not defined}\right\}, \quad (9)$$

as the set wherein $V(\cdot,\cdot)$ is not differentiable.

Theorem 1 ([11, p. 63]) *Let $V : [t_0,\infty) \times \mathcal{D} \to \mathbb{R}$ be Lipschitz continuous. The Clarke gradient of $V(\cdot,\cdot)$ at $(t,x) \in [t_0,\infty) \times \mathcal{D}$ is given by*

$$\partial V(t,x) = \overline{\mathrm{co}}\left\{\lim_{i\to\infty}\left[\frac{\partial V(t_i,x_i)}{\partial t}, \frac{\partial V(t_i,x_i)}{\partial x}\right]^{\mathrm{T}} : (t_i,x_i) \to (t,x), \; (t_i,x_i) \notin \Omega_V, x_i \notin \mathcal{N}, i \in \mathbb{N}\right\}, \quad (t,x) \in [t_0,\infty) \times \mathcal{D}, \quad (10)$$

where $\mathcal{N} \subset \mathcal{D}$ is an arbitrary set of measure zero.

Next, we recall a result that characterizes the total derivative of a Lipschitz continuous, regular function. For the statement of this result, consider the nonlinear, time-varying dynamical system

$$\dot{x}(t) = f(t,x(t)), \quad x(t_0) = x_0, \quad t \geq t_0, \quad (11)$$

where $f : [t_0,\infty) \times \mathcal{D} \to \mathbb{R}^n$ is such that $f(\cdot,x)$ is Lebesgue integrable and essentially locally bounded uniformly in $t \in [t_0,\infty)$ for all $x \in \mathcal{D}$ and $f(t,\cdot)$ is continuous in x uniformly in t for all t in compact subsets of $[t_0,\infty)$.

Lemma 1 ([17]) *Let $x : [t_0,\infty) \to \mathcal{D}$ denote a solution of Eq. 11 in the sense of Filippov and let $V : [t_0,\infty) \times \mathcal{D} \to \mathbb{R}$ be Lipschitz continuous and regular. Then $V(t,x(t))$, $t \geq t_0$, is absolutely continuous, $\dot{V}(t,x(t))$ exists almost everywhere on $[t_0,\infty)$, and $\dot{V}(t,x(t)) \in \dot{\overline{V}}(t,x(t))$, $t \in [t_0,\infty)$ a.e., where*

$$\dot{\overline{V}}(t,x) \triangleq \bigcap_{\xi \in \partial V(t,x)} \xi^{\mathrm{T}} \begin{bmatrix} K[f](t,x) \\ 1 \end{bmatrix}, \quad (t,x) \in [t_0,\infty) \times \mathcal{D}. \quad (12)$$

The next result, which is a direct consequence of Corollary 1 of [17], guarantees that maximal solutions of Eq. 1 in the sense of Filippov are defined on $\mathcal{I} = [t_0,\infty)$, and provides a generalization of the LaSalle-Yoshizawa theorem [19, Th. 4.7]. For the statement of this result, let $f : [t_0,\infty) \times \mathcal{D} \to \mathbb{R}^n$ be so that $f_{\sigma(t)}(t,x) = f(t,x)$, $(t,x) \in [t_0,\infty) \times \mathcal{D}$, and the nonlinear differential equation under time-dependent switching (1) is equivalent to the nonlinear, time-varying, discontinuous dynamical system (11).

Theorem 2 *Consider the nonlinear, discontinuous dynamical systems (1) and (11). Let $r > 0$ be such that $\mathcal{B}_r(0) \subset \mathcal{D}$, let $V : [t_0,\infty) \times \mathcal{D} \to \mathbb{R}$ be Lipschitz continuous and regular, let $W_1, W_2, W_3 : \mathcal{D} \to \mathbb{R}$ be such that both $W_1(\cdot)$ and $W_2(\cdot)$ are positive-definite and $W_3(\cdot)$ is nonnegative-definite, and let $c \in \left(0, \min_{\partial\mathcal{B}_r(0)} W_1(x)\right)$. If*

$$W_1(x) \leq V(t,x) \leq W_2(x), \qquad (t,x) \in [t_0,\infty) \times \mathcal{D}, \quad (13)$$

$$\dot{V}(t,x(t)) \leq -W_3(x(t)), \qquad t \geq t_0 \;\; a.e., \quad (14)$$

where $x(\cdot)$ denotes a maximal solution of Eq. 11 in the sense of Filippov such that $x(t_0) \in \{x \in \mathcal{B}_r(0) : W_2(x) \leq c\}$, then $x : [t_0,\infty) \to \mathcal{D}$ is bounded and such that $\lim_{t\to\infty} W_3(x(t)) = 0$. Furthermore, if $\mathcal{D} = \mathbb{R}^n$ and both $W_1(\cdot)$ and $W_2(\cdot)$ are radially unbounded, then every maximal solution $x(\cdot)$ of the Filippov regularization of Eq. 11 is bounded uniformly in both $t_0 \in [0,\infty)$ and $\sigma(\cdot)$, and such that $\lim_{t\to\infty} W_3(x(t)) = 0$ for all $x_0 \in \mathbb{R}^n$ uniformly in both t_0 and $\sigma(\cdot)$.

It is worthwhile to note that Theorem 2 does not involve any condition on the dwell-time of the nonlinear dynamical system (1), that is, on the minimal time interval between any pair of consecutive switching times [36, p. 56], but relies on the assumption that the switching signal $\sigma(\cdot)$ has countably many discontinuities. As discussed in Remark 1 of [26], if $\sigma(\cdot)$ is Lebesgue measurable, but does not have countably many discontinuities, then Theorem 2 of [26] provides an alternative to Theorem 2 above.

3 Model Reference Adaptive Control of Switched Dynamical Systems

3.1 Problem formulation

In this section, we design an adaptive control law for unknown nonlinear plants, whose dynamics are captured by time-dependent switching among multiple models, so that their trajectories mimic the trajectories of user-defined reference models under time-dependent switching.

Specifically, consider the nonlinear *plant* under time-dependent switching

$$\dot{x}(t) = A_{\sigma(t)}x(t) + B_{\sigma(t)}\left[u(t) + \Theta^{\mathrm{T}}\Phi_{\sigma(t)}(t,x(t))\right], \quad x(t_0) = x_0, \quad t \geq t_0, \quad (15)$$

where $x(t) \in \mathcal{D}$, $t \geq t_0 \geq 0$, denotes the *plant's trajectory*, $u(t) \in \mathbb{R}^m$ denotes the *control input*, the set $\mathcal{D} \subseteq \mathbb{R}^n$ is open, connected, and such that $0 \in \mathcal{D}$, $\sigma : [t_0,\infty) \to \Sigma$ denotes the switching signal and is user-defined, $\Sigma \subset \mathbb{N}$ is bounded, $A_s \in \mathbb{R}^{n\times n}$ is unknown, $s \in \Sigma$, $B_s \in \mathbb{R}^{n\times m}$ is known, $\Theta \in \mathbb{R}^{N\times m}$ is unknown, the *regressor vector* $\Phi_s : [t_0,\infty) \times \mathbb{R}^n \to \mathbb{R}^N$ is known, Lebesgue integrable,

and jointly continuous in its arguments, and $\Phi_s(t,\cdot)$ is Lipschitz continuous in x uniformly in t on compact subsets of $[t_0,\infty)$. Without loss of generality, we assume that Σ comprises the first $\overline{\sigma}$ positive integers, where $\overline{\sigma}$ denotes the cardinality of Σ.

The unknown matrix A_s, $s \in \Sigma$, in Eq. 15 captures *parametric uncertainties*, and the mapping $s \mapsto A_s$ is considered as unknown. We assume that the pairs (A_s, B_s) are controllable for all $s \in \Sigma$; although the entries of A_s are unknown, this hypothesis can be verified in problems of practical interest since the structure of A_s is usually known [33, p. 281].

The term $\Theta^{\mathrm{T}}\Phi_s(t,x)$, $(s,t,x) \in \Sigma \times [t_0,\infty) \times \mathbb{R}^n$, in Eq. 15 captures *matched uncertainties*. Matched uncertainties may be equivalently captured by $\bar{\Theta}_{\sigma(t)}^{\mathrm{T}}\bar{\Phi}_{\sigma(t)}(t,x)$, $(t,x) \in [t_0,\infty) \times \mathbb{R}^n$, where $\bar{\Theta}_s \in \mathbb{R}^{\bar{N}_s \times m}$, $s \in \Sigma$, is unknown, the mapping $s \mapsto \bar{\Theta}_s$ is unknown, and $\bar{\Phi}_s : [t_0,\infty) \times \mathbb{R}^n \to \mathbb{R}^{\bar{N}_s}$ is known. However, there always exist $\Theta \in \mathbb{R}^{N \times m}$ and a *regressor vector* $\Phi_s : [t_0,\infty) \times \mathbb{R}^n \to \mathbb{R}^N$, $s \in \Sigma$ such that $\Theta^{\mathrm{T}}\Phi_{\sigma(t)}(t,x) = \bar{\Theta}_{\sigma(t)}^{\mathrm{T}}\bar{\Phi}_{\sigma(t)}(t,x)$, $t \geq t_0$. Indeed, let $\Sigma_1, \ldots, \Sigma_p \subseteq \Sigma$, $p \leq \overline{\sigma}$, denote partitions of Σ. Uncertainties in the mapping $s \mapsto \bar{\Theta}_s$ can be captured by designing Σ_j, $j = 1, \ldots, p$, as a non-singleton set, and the dynamical model (15) can be deduced by setting $\Phi_s(t,x) = \left[\mathbf{1}_{\Sigma_1}(s)\bar{\Phi}_1^{\mathrm{T}}(t,x), \ldots, \mathbf{1}_{\Sigma_p}(s)\bar{\Phi}_p^{\mathrm{T}}(t,x)\right]^{\mathrm{T}}$, $(s,t,x) \in \Sigma \times [t_0,\infty) \times \mathbb{R}^n$, $\Theta = \left[\bar{\Theta}_1^{\mathrm{T}}, \ldots, \bar{\Theta}_p^{\mathrm{T}}\right]^{\mathrm{T}}$, and $N = \sum_{j=1}^{p} \bar{N}_j$. Regressor vectors are usually designed leveraging on prior knowledge of the plant dynamics [33, Ch. 9].

Consider also the *reference dynamical model* under time-dependent switching

$$\begin{aligned} \dot{x}_{\mathrm{ref}}(t) &= A_{\mathrm{ref},\sigma(t)}x_{\mathrm{ref}}(t) + B_{\mathrm{ref},\sigma(t)}r(t), \\ x_{\mathrm{ref}}(t_0) &= x_{\mathrm{ref},0}, \qquad t \geq t_0, \end{aligned} \tag{16}$$

where the $x_{\mathrm{ref}}(t) \in \mathbb{R}^n$, $t \geq t_0$, denotes the *reference trajectory*, the *reference command input* $r(t) \in \mathbb{R}^m$ is piecewise continuous and bounded, $A_{\mathrm{ref},s} \in \mathbb{R}^{n \times n}$ is Hurwitz, $s \in \Sigma$, and $B_{\mathrm{ref},s} \in \mathbb{R}^{n \times m}$, and assume there exist pairs $(K_{x,s}, K_{r,s}) \in \mathbb{R}^{n \times m} \times \mathbb{R}^{m \times m}$ such that the *matching conditions*

$$A_{\mathrm{ref},s} = A_s + B_s K_{x,s}^{\mathrm{T}}, \qquad s \in \Sigma, \tag{17}$$

$$B_{\mathrm{ref},s} = B_s K_{r,s}^{\mathrm{T}}, \tag{18}$$

are verified. In the following, we assume that the reference dynamical model (16) is input-to-state stable. This assumption is realistic since each linear, time-invariant, dynamical system comprised in the switched reference model (16) is input-to-state stable and hence, there exists a dwell-time such that Eq. 16 is input-to-state stable [62].

Lastly, assume there exists a symmetric positive-definite matrix $P \in \mathbb{R}^{n \times n}$ that verifies the set of Lyapunov matrix inequalities

$$A_{\mathrm{ref},s}^{\mathrm{T}}P + PA_{\mathrm{ref},s} < 0, \qquad s \in \Sigma, \tag{19}$$

and consider the *trajectory tracking error dynamics*

$$\begin{aligned} \dot{e}(t) &= A_{\mathrm{ref},\sigma(t)}e(t) + B_{\sigma(t)}\Delta\Theta^{\mathrm{T}}(t)\tilde{\Phi}_{\sigma(t)}(t,x(t)), \\ e(t_0) &= x_0 - x_{\mathrm{ref},0}, \quad t \geq t_0, \end{aligned} \tag{20}$$

and the *adaptive law*

$$\dot{\hat{\Theta}}(t) = -\Gamma\tilde{\Phi}_{\sigma(t)}(t,x(t))e^{\mathrm{T}}(t)PB_{\sigma(t)}, \quad \hat{\Theta}(t_0) = \hat{\Theta}_0, \tag{21}$$

where $\hat{\Theta} : [t_0,\infty) \to \mathbb{R}^{(\overline{\sigma}(n+m)+N)\times m}$ denotes the *adaptive gain*, $\Delta\Theta(t) \triangleq \hat{\Theta}(t) - \tilde{\Theta}$,

$$\tilde{\Phi}_s(t,x) \triangleq \begin{bmatrix} \mathcal{I}(s) \otimes x \\ \mathcal{I}(s) \otimes r(t) \\ -\Phi_s(t,x) \end{bmatrix}, \quad (s,t,x) \in \Sigma \times [t_0,\infty) \times \mathbb{R}^n, \tag{22}$$

$$\mathcal{I}(s) \triangleq \left[\mathbf{1}_{\{s\in\Sigma : s-1=0\}}(s), \ldots, \mathbf{1}_{\{s\in\Sigma : s-\overline{\sigma}=0\}}(s)\right]^{\mathrm{T}}, \tag{23}$$

$$\tilde{\Theta} \triangleq \left[K_{x,1}^{\mathrm{T}}, \ldots, K_{x,\overline{\sigma}}^{\mathrm{T}}, K_{r,1}^{\mathrm{T}}, \ldots, K_{r,\overline{\sigma}}^{\mathrm{T}}, \Theta^{\mathrm{T}}\right]^{\mathrm{T}}, \tag{24}$$

$x(\cdot)$ verifies (15) with $u(t) = \phi(\hat{\Theta}(t), \tilde{\Phi}_{\sigma(t)}(t,x(t)))$,

$$\begin{aligned} &\phi(\hat{\Theta}, \tilde{\Phi}_s) = \hat{\Theta}^{\mathrm{T}}\tilde{\Phi}_s, \\ &(s, \hat{\Theta}, \tilde{\Phi}_s) \in \Sigma \times \mathbb{R}^{(\overline{\sigma}(n+m)+N)\times m} \times \mathbb{R}^{\overline{\sigma}(n+m)+N}, \end{aligned} \tag{25}$$

denotes the *control law*, and $\Gamma \in \mathbb{R}^{(\overline{\sigma}(n+m)+N)\times(\overline{\sigma}(n+m)+N)}$ is symmetric and positive-definite, and denotes the *adaptive rate matrix*.

Our goal is to prove that solutions of both (20) and (21) are bounded uniformly in $t_0 \in [0,\infty)$ and $\sigma(\cdot)$ and that solutions of Eq. 20 converge asymptotically to zero uniformly in t_0 and $\sigma(\cdot)$. Since both (20) and (21) are discontinuous, multiple notions of solutions may be applied [13]. In this paper, we consider two classes of absolutely continuous [50, p. 127] generalized solutions of Eqs. 20 and 21, namely Carathéodory and Filippov solutions.

In the Carathéodory framework, it can be verified that if $x(\cdot)$ denotes the solution of Eq. 15 with $u(t) = \phi(\hat{\Theta}(t), \tilde{\Phi}_{\sigma(t)})$, $t \geq t_0$, and $x_{\mathrm{ref}}(\cdot)$ denotes the solution of (16), then the solution $e(\cdot)$ of Eq. 20 is such that $e(t) = x(t) - x_{\mathrm{ref}}(t)$, $t \geq t_0$ a.e.

However, a solution $e(\cdot)$ of Eq. 20 in the sense of Filippov is not necessarily equivalent to the difference of a solution $x(\cdot)$ of Eq. 15 with $u(t) = \phi(\hat{\Theta}(t), \tilde{\Phi}_s(t))$, $t \geq t_0$, and a solution $x_{\mathrm{ref}}(\cdot)$ of Eq. 16. If $x(t) = x_{\mathrm{ref}}(t)$, $t \geq T$ a.e., for some $T \geq t_0$, and $e(t) = 0$, then this equivalence can be established for all $t \geq T$ a.e.; for details, see [49].

In the following, $n_{\mathrm{d}}(t,t_0) \in \mathbb{N}$ denotes the *number of discontinuities of* $\sigma(\cdot)$ *over the interval* (t_0,t), $\mathcal{T}_{\sigma(t)} \triangleq \{\tau_j \in [t_0,t) : \sigma(\cdot)$ is discontinuous at τ_j, $j = 0, \ldots, n_{\mathrm{d}}(t,t_0)\}$ denotes the totally ordered *set of switching times over* $[t_0,t)$, and we set $t_0 = \tau_0 \in \mathcal{T}_{\sigma(t)}$ so that both $A_{\mathrm{ref},\sigma(\cdot)}$

and $B_{\mathrm{ref},\sigma(\cdot)}$ are constant between switching times, that is, $(A_{\mathrm{ref},\sigma(\mu)}, B_{\mathrm{ref},\sigma(\mu)}) = (A_{\mathrm{ref},\sigma(\tau_j)}, B_{\mathrm{ref},\sigma(\tau_j)})$ for all $\mu \in [\tau_j, \tau_{j+1}) \cap [t_0, t)$ and for all $j = 0, \ldots, n_{\mathrm{d}}(t, t_0)$, where $\tau_j \in \mathcal{T}_{\sigma(t)}$ and $(A_{\mathrm{ref},\sigma(\tau_j)}, B_{\mathrm{ref},\sigma(\tau_j)}) = \lim_{\tau\to 0^+}(A_{\mathrm{ref},\sigma(\tau_j+\tau)}, B_{\mathrm{ref},\sigma(\tau_j+\tau)})$. For simplicity of notation, we define $\mathcal{T} \triangleq \lim_{t\to\infty} \mathcal{T}_{\sigma(t)}$.

3.2 Carathéodory framework

In this section, we address the model reference adaptive control design problem posed in Section 3.1 by analyzing Carathéodory solutions of the trajectory tracking error dynamics (20) and the adaptive law (21) and assuming that the switching signal $\sigma(\cdot)$ is piece-wise constant and such that $\sigma(t) = \lim_{\tau\to t^+}\sigma(\tau)$ for each $\tau \geq t_0$. It is worthwhile to note that the switched dynamical system given by Eqs. 20 and 21 is continuous in $t \in [\tau_{j-1}, \tau_j)$ for all $(j, \tau_{j-1}, e, \hat{\Theta}) \in \mathbb{N} \times \mathcal{T} \times \mathbb{R}^n \times \mathbb{R}^{(\overline{\sigma}(n+m)+N)\times m}$ and locally Lipschitz continuous in $(e, \hat{\Theta})$ uniformly in t for all t in compact subsets of $[t_0, \infty)$, and hence it follows from Theorem 1.2 of [16] that there exists a unique pair $(e, \hat{\Theta}) : [t_0, \infty) \to \mathbb{R}^n \times \mathbb{R}^{(\overline{\sigma}(n+m)+N)\times m}$ that verifies (20) and (21) in the sense of Carathéodory.

The next theorem is the main result of this section and proves that if the trajectory tracking error $e(\cdot)$ and the adaptive gain matrix $\hat{\Theta}(\cdot)$ verify (20) and (21), respectively, in the sense of Carathéodory, then both the trajectory tracking error and the adaptive gain matrix are uniformly bounded, and the closed-loop plant's trajectory asymptotically converges to the reference model's trajectory. To prove this result, it is worthwhile to recall the following generalization of Barbalat's lemma [27, Lemma 8.2] and that the *dwell-time* $t_{\mathrm{d}} \triangleq \inf\{|\tau_j - \tau_{j-1}| : \tau_{j-1} \in \mathcal{T}, j \in \mathbb{N}\}$ of the switching signal $\sigma(\cdot)$ captures the length of the minimal interval between switching times [36, p. 56].

Lemma 2 ([24]) *Let $h : [t_0, \infty) \to \mathbb{R}$ be piece-wise continuously differentiable and let $\{t_k\}_{k=1}^{\infty} \subset [t_0, \infty)$ denote the sequence of points of discontinuity of $h(\cdot)$. Suppose that $\inf_{k\in\mathbb{N}} |t_k - t_{k-1}| > 0$ and that both $h(\cdot)$ and $\dot{h}(\cdot)$ are bounded on $[t_{k-1}, t_k)$ uniformly in $k \in \mathbb{N}$. If $\lim_{t\to\infty}\int_0^t h(\tau)\mathrm{d}\tau$ exists and is finite, then $\lim_{t\to\infty} h(t) = 0$ uniformly in $k \in \mathbb{N}$.*

Theorem 3 *Consider the closed-loop trajectory tracking error dynamics (20) and the adaptive law (21). Assume that the matching conditions (17) and (18) are verified, $t_{\mathrm{d}} > 0$, and there exist symmetric positive-definite matrices $P, Q \in \mathbb{R}^{n\times n}$ so that*

$$A_{ref,s}^{\mathrm{T}} P + P A_{ref,s} < -Q. \qquad s \in \Sigma. \tag{26}$$

Then, both the trajectory tracking error $e(\cdot)$ and the adaptive gain matrix $\hat{\Theta}(\cdot)$ are bounded uniformly in both $t_0 \in [0, \infty)$ and $\sigma(\cdot)$, and $e(t) \to 0$ as $t \to \infty$ uniformly in both t_0 and $\sigma(\cdot)$.

Proof Consider the common Lyapunov function candidate

$$V(t, e, \Delta\Theta) = e^{\mathrm{T}} P e + \mathrm{tr}\left(\Delta\Theta^{\mathrm{T}}\Gamma^{-1}\Delta\Theta\right),$$
$$(t, e, \Delta\Theta) \in [t_0, \infty) \times \mathbb{R}^n \times \mathbb{R}^{(\overline{\sigma}(n+m)+N)\times m}, \tag{27}$$

and note that if there exist symmetric positive-definite matrices $P, Q \in \mathbb{R}^{n\times n}$ so that Eq. 26 is verified, then the Lyapunov inequality (19) is verified. Next, it follows from Eqs. 27 and 26 that

$$\begin{aligned}
&\dot{V}(t, e(t), \Delta\Theta(t)) \\
&\leq -\alpha_{\min}\|e(t)\|^2 + 2e^{\mathrm{T}}(t) P B_{\sigma(t)} \Delta\Theta^{\mathrm{T}}(t)\tilde{\Phi}_{\sigma(t)}(t, x(t)) \\
&\quad +2\mathrm{tr}\left(\Delta\Theta^{\mathrm{T}}(t)\Gamma^{-1}\dot{\hat{\Theta}}(t)\right) \\
&= -\alpha_{\min}\|e(t)\|^2 \\
&\quad +2\mathrm{tr}\left(\Delta\Theta^{\mathrm{T}}(t)\left[\Gamma^{-1}\dot{\hat{\Theta}}(t) + \tilde{\Phi}_{\sigma(t)}(t, x(t)) e^{\mathrm{T}}(t) P B_{\sigma(t)}\right]\right) \\
&= -\alpha_{\min}\|e(t)\|^2, \quad t \geq t_0 \ \text{ a.e.},
\end{aligned} \tag{28}$$

along the trajectories of Eqs. 20 and 21, where $\alpha_{\min} \triangleq \lambda_{\min}(Q)$.

Since both $V(\cdot,\cdot,\cdot)$ and $\dot{V}(\cdot,\cdot,\cdot)$ do not explicitly depend on t and $\sigma(\cdot)$ and $\dot{V}(t, e(t), \Delta\Theta(t))$, $t \geq t_0$, is a non-increasing function of time, by proceeding as in Theorem 4.13 of [19] it can be proven that both $e(\cdot)$ and $\hat{\Theta}(\cdot)$ are bounded on $[\tau_{j-1}, \tau_j)$ uniformly in $j \in \mathbb{N}$ for all $\tau_j \in \mathcal{T}$.

Next, since $V(t, e, \Delta\Theta)$, $(t, e, \Delta\Theta) \in [t_0, \infty) \times \mathbb{R}^n \times \mathbb{R}^{(\overline{\sigma}(n+m)+N)\times m}$, is positive-definite and $\dot{V}(t, e(t), \Delta\Theta(t))$ is non-positive definite, it follows from the monotone convergence theorem [19, Th. 2.10] that there exists $V_e \geq 0$ such that $V(t, e(t), \Delta\Theta(t)) \to V_e$ as $t \to \infty$. Moreover, $\dot{x}_{\mathrm{ref}}(\cdot)$ is bounded on $[\tau_{j-1}, \tau_j)$ uniformly in $j \in \mathbb{N}$ for all $\tau_{j-1} \in \mathcal{T}$ since $A_{\mathrm{ref},s}$, $s \in \Sigma$, is Hurwitz, Σ is bounded, and $r(\cdot)$ is bounded. Furthermore, since Σ is bounded, it follows from Eqs. 25 and 15 with $u(t) = \phi(\hat{\Theta}(t), \tilde{\Phi}_{\sigma(t)}(t))$ that $\dot{x}(\cdot)$ is bounded on $[\tau_{j-1}, \tau_j)$ uniformly in $j \in \mathbb{N}$ for all $\tau_{j-1} \in \mathcal{T}$. Therefore, $\dot{e}(\cdot)$ is bounded on $[\tau_{j-1}, \tau_j)$ uniformly in $j \in \mathbb{N}$ for all $\tau_{j-1} \in \mathcal{T}$ and $\ddot{V}(t, e(t), \hat{K}(t), \hat{K}_g(t)) = -2e^{\mathrm{T}}(t) Q \dot{e}(t)$ is bounded on $[\tau_{j-1}, \tau_j)$ uniformly in $j \in \mathbb{N}$ for all $\tau_{j-1} \in \mathcal{T}$. Consequently, it follows from Lemma 2 that $\dot{V}(t, e(t), \hat{K}(t), \hat{K}_g(t)) \to 0$ as $t \to \infty$ and hence, it follows from (28) that $e(t) \to 0$ as $t \to \infty$ uniformly in $t_0 \in [0, \infty)$ and $\sigma(\cdot)$, which concludes the proof. □

Theorem 3 proves that if the matching conditions (17) and (18) are verified, the dwell-time t_{d} of the switching signal $\sigma(\cdot)$ is arbitrarily small, but non-zero, and there exists a solution to the Lyapunov inequality (19), then both the

trajectory tracking error $e(\cdot)$ and the adaptive gain matrix $\hat{\Theta}(\cdot)$ are bounded and the trajectory of the closed-loop plant (15) with $u(t) = \phi(\hat{\Theta}(t), \tilde{\Phi}_{\sigma(t)})$, $t \geq t_0$, eventually mimics the trajectory of the reference model (16), that is, $\lim_{t\to\infty} \|e(t)\| = \lim_{t\to\infty} \|x(t) - x_{\mathrm{ref}}(t)\| = 0$ uniformly in both $t_0 \in [0, \infty)$ and $\sigma(\cdot)$.

3.3 Filippov Framework

In this section, we address the model reference adaptive control design problem posed in Section 3.1 by analyzing Filippov solutions of the trajectory tracking error dynamics (20) and the adaptive law (21) and assuming that the switching signal $\sigma(\cdot)$ is Lebesgue integrable and has countably many points of discontinuity over the time interval $[t_0, \infty)$. To this goal, define the *vectorized adaptive gain* $\hat{\theta}(t) \triangleq \mathrm{vec}(\hat{\Theta}(t))$, $t \geq t_0$, where $\mathrm{vec}(\cdot)$ denotes the vector-stacking operator, and consider the *vectorized adaptive law*

$$\begin{aligned} &\dot{\hat{\theta}}(t) = -\mathrm{vec}\left(\Gamma \tilde{\Phi}_{\sigma(t)}(t, x(t)) e^{\mathrm{T}}(t) P B_{\sigma(t)}\right), \\ &\hat{\theta}(t_0) = \mathrm{vec}(\hat{\Theta}_0), \qquad t \geq t_0, \end{aligned} \tag{29}$$

which has been deduced from Eq. 21. Furthermore, let $y(t) \triangleq \left[e^{\mathrm{T}}(t), \hat{\theta}^{\mathrm{T}}(t)\right]^{\mathrm{T}}$, $t \geq t_0$, and

$$\begin{aligned} f(t, y) \triangleq &\begin{bmatrix} A_{\mathrm{ref},\sigma(t)} e + B_{\sigma(t)} \Delta \Theta^{\mathrm{T}} \tilde{\Phi}_{\sigma(t)}(t, x(t)) \\ -\mathrm{vec}\left(\Gamma \tilde{\Phi}_{\sigma(t)}(t, x(t)) e^{\mathrm{T}} P B_{\sigma(t)}\right) \end{bmatrix} \\ &(t, y) \in [t_0, \infty) \times \mathbb{R}^{n+m(\overline{\sigma}(n+m)+N)}, \end{aligned} \tag{30}$$

so that Eqs. 20 and 21 are equivalent to

$$\dot{y}(t) = f(t, y(t)), \quad y(t_0) = \begin{bmatrix} x_0 - x_{\mathrm{ref},0} \\ \mathrm{vec}(\hat{\Theta}_0) \end{bmatrix}, \quad t \geq t_0. \tag{31}$$

It is worthwhile to note that the nonlinear, discontinuous dynamical system given by Eq. 31 is Lebesgue integrable and essentially locally bounded uniformly in $t \in [t_0, \infty)$ since $\Phi_s(\cdot, \cdot)$ is Lebesgue integrable, continuous in $t \in [t_0, \infty)$, and Lipschitz continuous in $x \in \mathcal{D}$, uniformly in t for all $s \in \Sigma$, and $\sigma(\cdot)$ is Lebesgue integrable and bounded.

Theorem 4 *Consider the closed-loop trajectory tracking error dynamics* (20) *and the adaptive law* (21). *Assume that the matching conditions* (17) *and* (18) *are verified and there exist symmetric positive-definite matrices* $P, Q \in \mathbb{R}^{n\times n}$ *so that* (26) *is verified. Then, every maximal solution of the Filippov regularization of Eqs. 20 and 21 is bounded uniformly in both* $t_0 \in [0, \infty)$ *and* $\sigma(\cdot)$ *and such that* $e(t) \to 0$ *as* $t \to \infty$ *uniformly in both* t_0 *and* $\sigma(\cdot)$.

Proof Consider the candidate common Lyapunov function

$$\begin{aligned} &V(t, y) = e^{\mathrm{T}} P e + \tilde{\theta}^{\mathrm{T}} \tilde{\theta}, \\ &(t, y) \in [t_0, \infty) \times \mathbb{R}^{n+m(\overline{\sigma}(n+m)+N)}, \end{aligned} \tag{32}$$

where $\tilde{\theta} \triangleq \mathrm{vec}\left(\Gamma^{-\frac{1}{2}} \Delta\Theta\right)$, and note that if there exists $Q \in \mathbb{R}^{n\times n}$ that is symmetric, positive-definite, and such that Eq. 26 is verified, then the Lyapunov inequality (19) is verified.

Since $V(\cdot, \cdot)$ is continuously differentiable, the Lyapunov function candidate (32) is Lipschitz continuous and regular, and it follows from Lemma 1 that $\dot{V}(t, y(t)) \in \dot{\overline{V}}(t, y(t))$, $t \in [t_0, \infty)$ a.e., where

$$\begin{aligned} &\dot{\overline{V}}(t, y) \triangleq \bigcap_{\xi \in \partial V(t,y)} \xi^{\mathrm{T}} \begin{bmatrix} K[f](t, y) \\ 1 \end{bmatrix}, \\ &(t, y) \in [t_0, \infty) \times \mathbb{R}^{n+m(\overline{\sigma}(n+m)+N)}, \end{aligned} \tag{33}$$

and $f(\cdot, \cdot)$ verifies (31). Furthermore, since $V(\cdot, \cdot)$ is continuously differentiable and does not depend on t explicitly, it holds that

$$\begin{aligned} &\dot{\overline{V}}(t, y) \subset \frac{\partial V(t, y)}{\partial y} K[f](t, y) \subset 2\left[e^{\mathrm{T}} P, \tilde{\theta}^{\mathrm{T}}\right] K[f](t, y), \\ &(t, y) \in [t_0, \infty) \times \mathbb{R}^{n+m(\overline{\sigma}(n+m)+N)}, \end{aligned} \tag{34}$$

and since $f(t, \cdot)$ is continuous for all $t \in [t_0, \infty)$ and $f(\cdot, y)$ is continuous between switching times for all $y \in \mathbb{R}^{n+m(\overline{\sigma}(n+m)+N)}$, it follows from Theorem 1 of [44] that $K[f](t, y) = \{f(t, y)\}$ for all $(t, y) \in \left([\tau_{j-1}, \tau_j) \cap [t_0, t)\right) \times \mathbb{R}^{n+m(\overline{\sigma}(n+m)+N)}$, where $\tau_j \in \mathcal{T}$ and $j \in \mathbb{N}$. Therefore, by proceeding as in the proof of Theorem 3, it holds that

$$\dot{\overline{V}}(t, y(t)) \leq -\alpha_{\min} \|e(t)\|, \qquad t \in [t_0, \infty) \ \text{ a.e.}, \tag{35}$$

where $\alpha_{\min} = \lambda_{\min}(Q)$. Since $V(\cdot, \cdot)$ is positive-definite and radially unbounded and $W_3(y) = \alpha_{\min}\|e\|$ is a nonnegative-definite function of its argument, it follows from Theorem 2 that every maximal solution $y(\cdot)$ of the Filippov regularization of Eq. 31 is bounded uniformly in both $t_0 \in [t_0, \infty)$ and $\sigma(\cdot)$ and such that $\lim_{t\to\infty} e(t) = 0$ uniformly in both t_0 and $\sigma(\cdot)$. □

Theorem 4 proves that applying the control law (25) and the adaptive law (21) or, equivalently, Eqs. 25 and 29, both the trajectory tracking error $e(\cdot)$ and the adaptive gain matrix $\hat{\Theta}(\cdot)$ are bounded, and $\lim_{t\to\infty} \|e(t)\| = 0$ uniformly in both $t_0 \in [0, \infty)$ and $\sigma(\cdot)$. Hence, it follows from the definition of limit that given $\varepsilon > 0$, there exists $T \geq t_0$ such that $\|e(t)\| < \varepsilon$ for $t \geq T$ a.e.. Theorem 3 proved a similar result, assuming that the dwell-time is non-zero. Theorem 4, instead, allows zero dwell-time. Moreover, Theorem 3 guarantees the existence of a unique solution of the trajectory tracking error and the adaptive gains

dynamics, whereas Theorem 4 guarantees the existence, but not the uniqueness, of a solution of Eqs. 20 and 21.

4 Illustrative Numerical Example

In this section, we provide a numerical example to demonstrate the effectiveness of both the control law (25) and the adaptive law (21) to guarantee that the trajectory $x(\cdot)$ of the plant (15) with $u(t) = \phi(\hat{\Theta}(t), \tilde{\Phi}_{\sigma(t)}(t))$, $t \geq t_0$, eventually tracks the trajectory $x_{\mathrm{ref}}(\cdot)$ of the reference model (16). Specifically, we consider a delta-wing aircraft, whose wings' morphing mechanism is able to modify the vehicle's aerodynamic and geometric properties sufficiently fast to be considered as instantaneous, and whose aerodynamic and geometric coefficients are unknown. The roll dynamics of this vehicle is captured by

$$\begin{aligned}\begin{bmatrix}\dot{\varphi}(t)\\ \dot{p}(t)\end{bmatrix} &= \begin{bmatrix}0 & 1\\ \theta_{1,\sigma(t)} & \theta_{2,\sigma(t)}\end{bmatrix}\begin{bmatrix}\varphi(t)\\ p(t)\end{bmatrix}\\ &\quad+\begin{bmatrix}0\\ \theta_{3,\sigma(t)}\end{bmatrix}\left[u(t)+\Theta^{\mathrm{T}}\Phi_{\sigma(t)}(t,\varphi(t),p(t))\right],\\ \begin{bmatrix}\varphi(0)\\ p(0)\end{bmatrix} &= \begin{bmatrix}\varphi_0\\ p_0\end{bmatrix}, \qquad t\geq 0,\end{aligned} \tag{36}$$

where $\varphi(\cdot)$ denotes the *roll angle*, $p(\cdot)$ denotes the *roll rate*, $u(\cdot)$ denotes the *roll moment*, $\theta_{1,s}, \theta_{2,s}, \theta_{3,s} \in \mathbb{R}$ capture aerodynamic coefficients of the aircraft, $s \in \Sigma$, $\Sigma = \{1, 2\}$, $\theta_{1,s}$ and $\theta_{2,s}$ are unknown, $\Theta \in \mathbb{R}^4$ is unknown,

$$\begin{aligned}&\Phi_s(t,\varphi,p)\\ &=\left[\mathbf{1}_{\{s\in\Sigma:s-1=0\}}(s)\bar{\Phi}_1(t,\varphi,p),\ \mathbf{1}_{\{s\in\Sigma:s-2=0\}}(s)\bar{\Phi}_2^{\mathrm{T}}(t,\varphi,p)\right]^{\mathrm{T}},\\ &(s,t,\varphi,p)\in\Sigma\times[t_0,\infty)\times\mathbb{R}\times\mathbb{R},\end{aligned}$$

denotes the regressor vector, and [33, pp. 285-291]

$$\begin{aligned}\bar{\Phi}_1(t,\varphi,p) &= \tanh\varphi,\\ \bar{\Phi}_2(t,\varphi,p) &= \left[|\varphi(t)|p(t),\ |p(t)|p(t),\ \varphi^3(t)\right]^{\mathrm{T}};\end{aligned}$$

note that Eq. 36 is in the same form as Eq. 15 with $n = 2$, $m = 1$, $t_0 = 0$, $x = [\varphi, p]^{\mathrm{T}}$, $A_s = \begin{bmatrix}0 & 1\\ \theta_{1,s} & \theta_{2,s}\end{bmatrix}$, $s \in \Sigma$, $\overline{\sigma} = 2$, and $B_s = \begin{bmatrix}0\\ \theta_{3,s}\end{bmatrix}$. Additionally, we consider the switched reference model (16) with $x_{\mathrm{ref}}(t) = [\varphi_{\mathrm{ref}}(t), p_{\mathrm{ref}}(t)]^{\mathrm{T}}$, $A_{\mathrm{ref},s} = \begin{bmatrix}0 & 1\\ -k_s & -c_s\end{bmatrix}$, $s \in \Sigma$, $k_s > 0$, $c_s > 0$, $B_{\mathrm{ref,\,s}} = \begin{bmatrix}0\\ b_s\end{bmatrix}$, and $b_s \in \mathbb{R}$ so that if $\sigma(t) = 1$, $t \geq 0$, then Eq. 16 captures a less responsive reference model, and if $\sigma(t) = 2$, then Eq. 16 captures a more responsive reference model. It is worthwhile to note that $A_{\mathrm{ref},s}$, $s \in \Sigma$, is in companion form and hence, there exists a symmetric positive-definite matrix $P \in \mathbb{R}^{2\times 2}$ that verifies (19) if and only if the matrix product $A_{\mathrm{ref},1}A_{\mathrm{ref},2}$ does not have any negative real eigenvalue [47].

Let $\theta_{1,1} = -9.15$, $\theta_{2,1} = -4.6$, $\theta_{3,1} = 1$, $\theta_{1,2} = -0.018$, $\theta_{2,2} = 0.015$, $\theta_{3,2} = 0.75$, $\Theta = [1, -0.062, 1, 0.009]^{\mathrm{T}}$, $k_1 = 1$, $c_1 = 3$, $b_1 = 1$, $k_2 = 150$, $c_2 = 45$, $b_2 = 150$, $r(t) = \frac{1}{2}\sin 2t$, $t \geq 0$, $\sigma(t) = \mathrm{rpi}\left(\frac{1}{2}\sin(\omega(t)t) + \frac{3}{2}\right)$, where $\mathrm{rpi}(\cdot)$ denotes the rounding function to the nearest integer,

$$\omega(t) = \begin{cases}0.5, & t\in[0,15)\cup[25,\infty),\\ \dfrac{3(t-15)}{4(25-t)}, & t\in[15,25),\end{cases}$$

$\Gamma = 50I_{10}$, $\varphi_0 = 1$, and $p_0 = 1$; note that the dwell-time converges to zero as $t \to 25$ from the left. In this case, $\mathrm{spec}(A_1) = \{-2.3000 - 1.9647\jmath, -2.3000 + 1.9647\jmath\}$ and $\mathrm{spec}(A_2) = \{0.0075 - 0.1340\jmath, 0.0075 + 0.1340\jmath, \}$, which implies that the uncontrolled plant is asymptotically stable for $s = 1$ and is unstable for $s = 2$. Furthermore, $\mathrm{spec}(A_{\mathrm{ref},1}A_{\mathrm{ref},2}) = \{-8.000 - 9.2736\jmath, -8.000 + 9.2736\jmath\}$, and Eq. 19 is verified by $P = \begin{bmatrix}2.99 & 0.75\\ 0.75 & 0.288\end{bmatrix}\cdot 10^4$.

Figure 1 shows plots of the aircraft's roll angle and the corresponding reference trajectory. The control law (25) and the adaptive law (21) guarantee satisfactory trajectory tracking despite uncertainties in the plant dynamics and the initial conditions and despite the arbitrarily small dwell-time over the interval [15, 25) s. Figure 2 shows a plot of the roll moment needed to track the reference trajectory. It is apparent that each switching is followed by a sudden increase of the control input, and over the time interval [15, 25) s, the control input is characterized by high-frequency oscillations due to the rapid sequence of switching times.

None of the control techniques for uncertain, switched, nonlinear plants that we surveyed is suitable to regulate (36). Therefore, to validate the usefulness of the adaptive law (21), we considered the problem of applying the control law (25) and the classical adaptive law

$$\begin{aligned}\dot{\hat{\Theta}}(t) &= -\Gamma\tilde{\Phi}_s(t,x(t))e^{\mathrm{T}}(t)PB_s, \quad s\in\Sigma,\\ \hat{\Theta}(t_0) &= \hat{\Theta}_0, \quad t\geq t_0,\end{aligned} \tag{37}$$

to regulate the aircraft's roll dynamics. If $s = 1$ in both (25) and (37), then the trajectory tracking error diverges. Alternatively, if $s = 2$ in both (25) and (37), then the aircraft is able to track the reference roll angle. However, as shown in Fig. 3, applying (25) and (37) with $s = 2$, the trajectory tracking error is consistently larger than the trajectory tracking error obtained by applying the proposed framework. Indeed, applying (25) and (21), the $\mathcal{L}_2$-norm of the trajectory tracking error is equal to 0.049N, and applying (25) and (37) with $s = 2$, the $\mathcal{L}_2$-norm of the

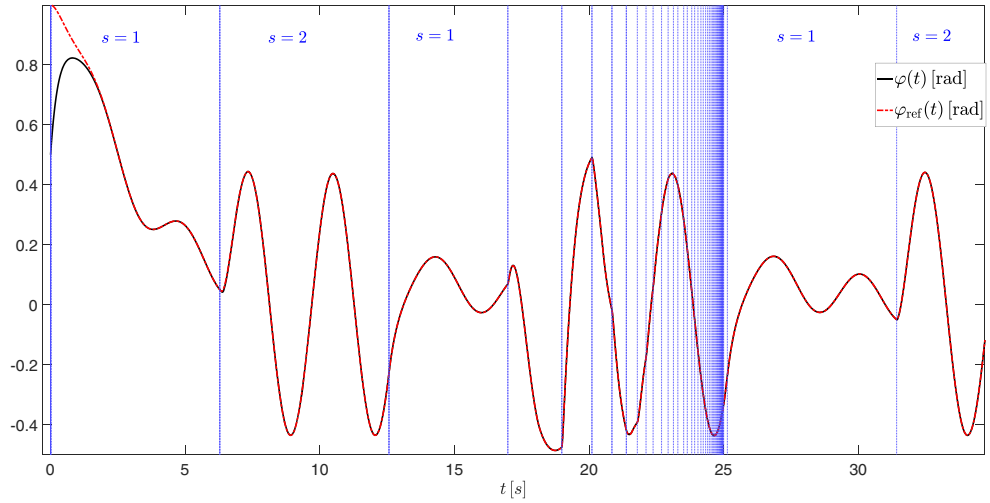

Fig. 1 Plot of the aircraft's roll angle $\varphi(\cdot)$ and reference roll angle $\varphi_{\text{ref}}(\cdot)$. The vertical lines mark the switching times. Despite the arbitrarily small dwell-time and the uncertainties in both the plant dynamics and the initial conditions, the aircraft's roll angle tracks closely the reference roll angle

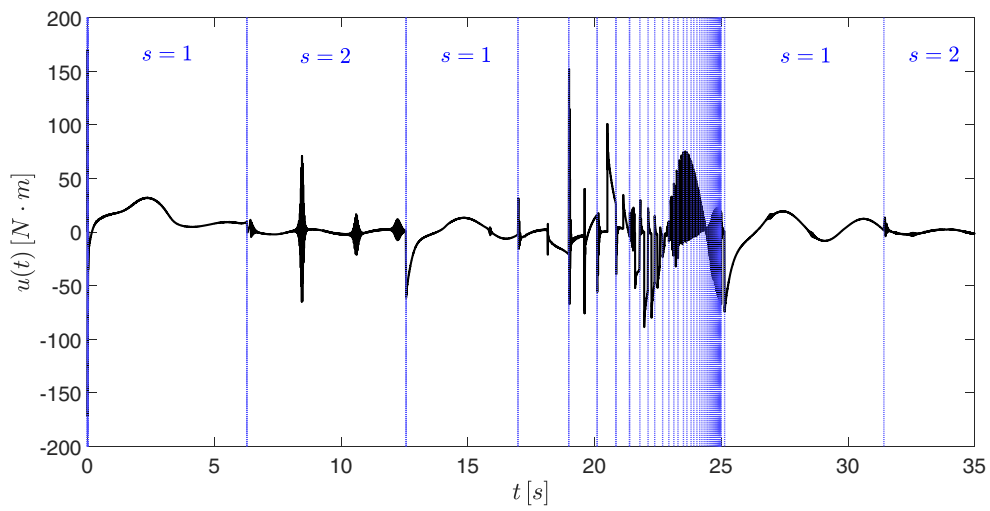

Fig. 2 Plot of control input obtained applying the control law (25) and the proposed adaptive law (21). Both the magnitude an the frequency of the control input increase with the frequency of the switching signal

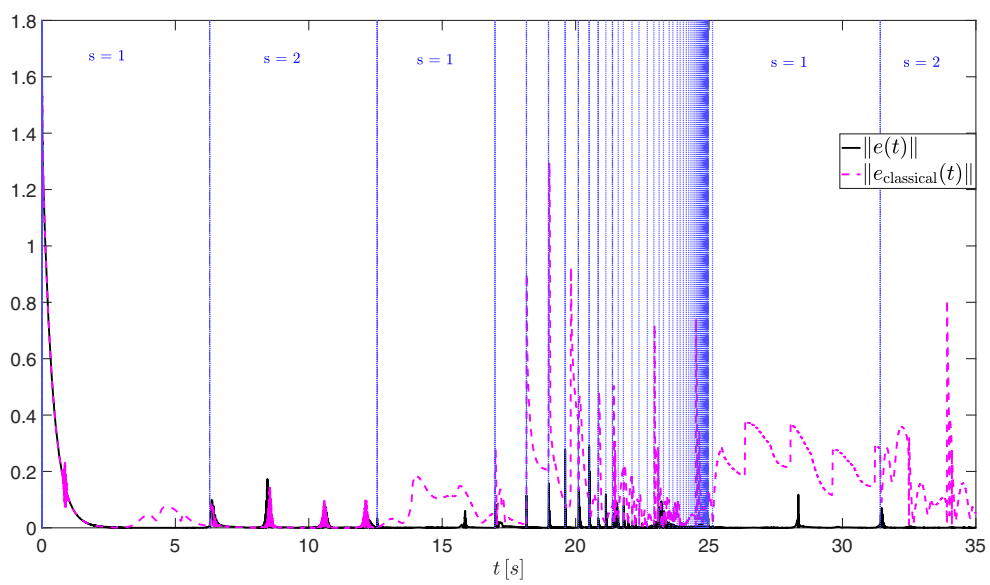

Fig. 3 Plot of the trajectory tracking error norm obtained by applying the control law (25) and the proposed adaptive law (21), namely $\|e(\cdot)\|$, and plot of the trajectory tracking error norm obtained by applying the control law (25) and the classical adaptive law (37) with $s = 2$, namely $\|e_{\text{classical}}(\cdot)\|$. Applying (25) and (21), the trajectory tracking error is consistently smaller

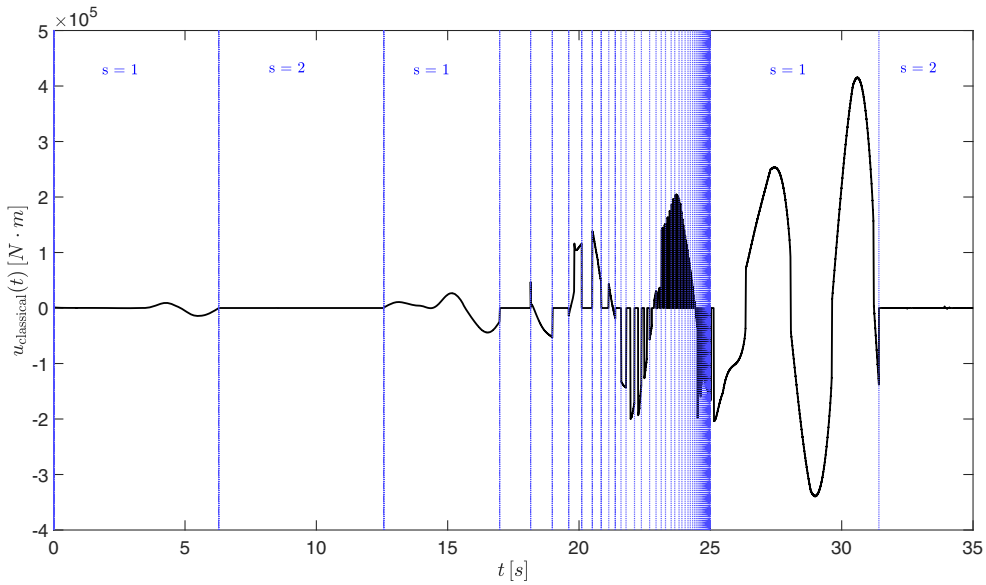

Fig. 4 Plot of control input obtained applying the control law (25) and the classical adaptive law (37) with $s = 2$. By comparing this plot with the plot in Fig. 2, it is apparent that applying (25) and (37) with $s = 2$, the control effort is three orders of magnitude larger than the control effort needed to apply (25) and (21)

trajectory tracking error is equal to 0.209N. Figure 4 shows the control input obtained applying (25) and (37) and $s = 2$. By comparing Figs. 2 and 4, it appears that applying (25) and (37) with $s = 2$, the control effort is three orders of magnitude larger than the control effort needed to apply (25) and (21); indeed, the $\mathcal{L}_\infty$-norm of the control input obtained by applying (25) and (37) with $s = 2$ is $415,559.07$N, whereas the $\mathcal{L}_\infty$-norm of the control input obtained applying (25) with the proposed adaptive law (21) is 171.75N. Lastly, we remark that, employing (25) and (21), the computational time is approximately 10.4 times shorter than employing (25) and (37) with $s = 2$.

5 Flight Tests

5.1 Problem Description

In order to validate the proposed model reference adaptive control framework for unknown switched nonlinear plants, we performed flight tests involving an aerial robot tasked with autonomously mounting a camera to a vertical surface. This aerial robot comprises a chassis, which is modeled as a rigid body, four propellers, whose spin axes can be tilted independently, a robotic arm, and a grasper, which comprises a suction cup mounted at the extremity of the robotic arm; for details, see Fig. 5. The camera is held by the grasper and is covered by one of the two sides of a linear fabric strip fastener. The point on the vertical surface where the camera must be installed is covered by the other side of the fabric strip fastener. After having exerted some normal force against the vertical surface and having engaged the fabric strip fastener, the suction cup is released and the aerial robot flies away from the vertical surface. A video of one of these flight tests can be found at [2].

5.2 Dynamical Modeling

To uniquely identify the position and orientation of the aerial robot in space, we consider two reference frames, namely the *inertial reference frame* $\mathbb{I} \triangleq \{O; X, Y, Z\}$ centered in $O \in \mathbb{R}^3$ and with orthonormal axes

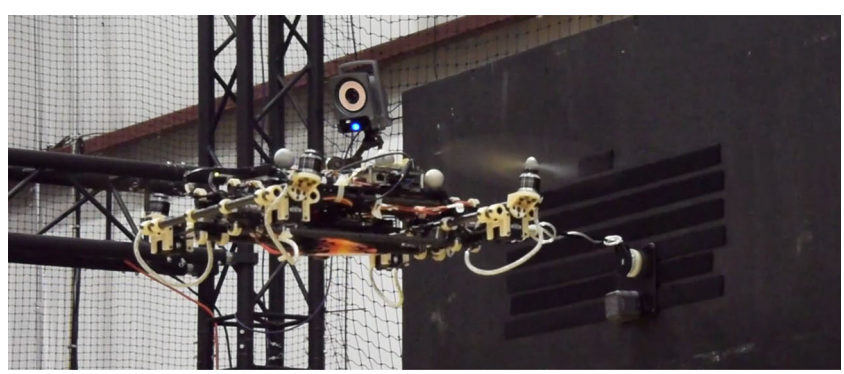

Fig. 5 Aerial robot installing a camera on a vertical surface. The camera is held by the grasper and is covered by one of the two sides of a linear fabric strip fastener. The vertical surface is partly covered by the other side of the fabric strip fastener so that, after having exerted some pressure against the vertical surface, the suction cup is released, and the aerial robot flies away

$X, Y, Z \in \mathbb{R}^3$ and the *body reference frame* $\mathbb{J}(\cdot) \triangleq \{A(\cdot); x(\cdot), y(\cdot), z(\cdot)\}$ centered at the extremity of the arm $A : [t_0, \infty) \to \mathbb{R}^3$ and with orthonormal axes $x, y, z : [t_0, \infty) \to \mathbb{R}^3$. If a vector $a \in \mathbb{R}^3$ is expressed in the reference frame $\mathbb{I}$, then it is denoted by $a^{\mathbb{I}}$; alternatively, if a vector is expressed in $\mathbb{J}(\cdot)$, then no superscript is used. The reference frame $\mathbb{I}$ is set so that the X axis is normal to the vertical surface and the force due to the gravitational acceleration is given by $F_{\mathrm{g}}^{\mathbb{I}} = -mgZ$, where $m > 0$ denotes the mass of the aerial robot and $g > 0$ denotes the gravitational acceleration. The reference frame $\mathbb{J}(\cdot)$ is set so that the propellers' arms are aligned to the $y(\cdot)$ axis; for details, see Fig. 6.

The position of the reference point $A(\cdot)$ with respect to O is denoted by $r_A^{\mathbb{I}} : [t_0, \infty) \to \mathbb{R}^3$ and the *velocity* of $A(\cdot)$ with respect to the reference frame $\mathbb{I}$ is denoted by $v_A^{\mathbb{I}} : [t_0, \infty) \to \mathbb{R}^3$. Using a 3-2-1 rotation sequence, the orientation of the body reference frame $\mathbb{J}(\cdot)$ with respect to the inertial reference frame $\mathbb{I}$ is captured by the *roll angle* $\phi : [t_0, \infty) \to [0, 2\pi)$, the *pitch angle* $\theta : [t_0, \infty) \to \left(-\frac{\pi}{2}, \frac{\pi}{2}\right)$, and the *yaw angle* $\psi : [t_0, \infty) \to [0, 2\pi)$ [31, pp. 11].

The *vector of independent generalized coordinates*

$$q(t) \triangleq \left[\left(r_A^{\mathbb{I}}(t)\right)^{\mathrm{T}}, \phi(t), \theta(t), \psi(t)\right]^{\mathrm{T}} \in \mathcal{D}, \quad t \geq t_0, \tag{38}$$

captures the position and orientation of $\mathbb{J}(\cdot)$ with respect to $\mathbb{I}$, where $\mathcal{D} \triangleq \mathbb{R}^3 \times \left(-\frac{\pi}{2}, \frac{\pi}{2}\right) \times \left(-\frac{\pi}{2}, \frac{\pi}{2}\right) \times [0, 2\pi)$. The *kinematic equations* of the aerial robot are given by

$$\dot{q}(t) = \begin{bmatrix} v_A^{\mathbb{I}}(t) \\ \Gamma(q(t))\omega(q(t), \dot{q}(t)) \end{bmatrix}, \quad q(t_0) = q_0, \quad t \geq t_0, \tag{39}$$

where $\omega : \mathcal{D} \times \mathbb{R}^6 \to \mathbb{R}^3$ denotes the *angular velocity* of the reference frame $\mathbb{J}(\cdot)$ with respect to $\mathbb{I}$, and [31, Th. 1.7]

$$\Gamma(q) \triangleq \begin{bmatrix} 1 & \sin\phi\tan\theta & \cos\phi\tan\theta \\ 0 & \cos\phi & -\sin\phi \\ 0 & \sin\phi\sec\theta & \cos\phi\sec\theta \end{bmatrix}, \quad q \in \mathcal{D};$$

it is worthwhile to recall that $\Gamma(q)$ is invertible, since $\theta \in \left(-\frac{\pi}{2}, \frac{\pi}{2}\right)$ [31, pp. 18-19].

After the fabric strip fastener has been engaged and before the suction cup is released, the point of contact between the robotic arm and the vertical surface is modeled as a cylindrical hinge since the aircraft can only rotate about the $y(\cdot)$ axis. Furthermore, the translation of the reference point $A(\cdot)$, the aircraft's roll angle, and the aircraft's yaw angle are impeded. Therefore, while the aerial robot is in contact with the vertical surface, the plant dynamics is in partial-state equilibrium [19, Def. 4.1]. Furthermore, the aerial robot's dynamics comprises two models, that is, $\Sigma = \{1, 2\}$. Specifically, the first model captures the aerial robot's free flight dynamics, and the state vector comprises twelve components, that is, the components of $[q^{\mathrm{T}}(\cdot), \dot{q}^{\mathrm{T}}(\cdot)]^{\mathrm{T}}$. The second dynamical model captures the aerial robot's pitch dynamics while in contact with the vertical surface, the state vector comprises two components, that is, $[\theta(\cdot), \dot{\theta}(\cdot)]^{\mathrm{T}}$, and the remaining components of $[q^{\mathrm{T}}(\cdot), \dot{q}^{\mathrm{T}}(\cdot)]^{\mathrm{T}}$ are at equilibrium. By proceeding as in [3], the translational and rotational dynamic equations of the aerial robot are given by

$$\begin{aligned} &\mathcal{H}_{\sigma(t)}\mathcal{M}(q(t)) \begin{bmatrix} \dot{v}_A^{\mathbb{I}}(t) \\ \dot{\omega}(q(t), \dot{q}(t)) \end{bmatrix} \\ &= \mathcal{H}_{\sigma(t)} \left(\begin{bmatrix} f_{\mathrm{dyn,\,tran}}(t, q(t), \dot{q}(t)) \\ f_{\mathrm{dyn,\,rot}}(t, q(t), \dot{q}(t)) \end{bmatrix} + G(q(t))u(t) \right), \\ &\left[v_A^{\mathbb{I},\mathrm{T}}(t_0), \omega^{\mathrm{T}}(t_0)\right]^{\mathrm{T}} = \left[v_{A,0}^{\mathbb{I},\mathrm{T}}, \omega_0^{\mathrm{T}}\right]^{\mathrm{T}}, \quad t \geq t_0, \end{aligned} \tag{40}$$

where

$$\mathcal{H}_s \triangleq \begin{bmatrix} \mathbf{1}_{\{s \in \Sigma : s-1=0\}}(s) I_3 & 0_{3\times 3} \\ 0_{3\times 3} & \mathcal{I}_{\mathrm{rot}}(s) \end{bmatrix}, \quad s \in \Sigma, \tag{41}$$

$$\mathcal{I}_{\mathrm{rot}}(s) \triangleq \mathrm{diag}\left(\mathbf{1}_{\{s \in \Sigma : s-1=0\}}(s), 1, \mathbf{1}_{\{s \in \Sigma : s-1=0\}}(s)\right),$$

$$\mathcal{M}(q) \triangleq \begin{bmatrix} mI_3 & -mR(q)r_C^{\times} \\ mr_C^{\times}R^{\mathrm{T}}(q) & \mathfrak{I} \end{bmatrix}, \quad q \in \mathcal{D}, \tag{42}$$

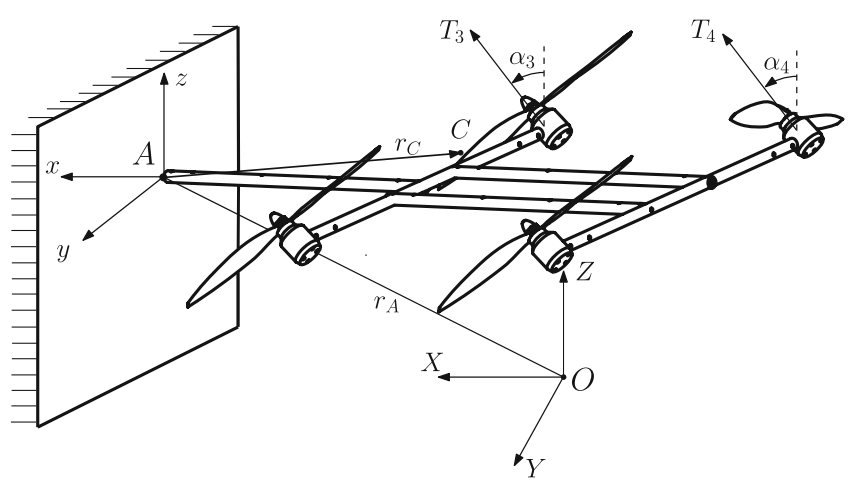

Fig. 6 Schematic representation of a simplified unmanned aerial manipulator system exerting a normal force against a vertical surface

denotes the *generalized mass matrix*, $r_C \in \mathbb{R}^3$ denotes the position of center of mass of the controlled mechanical system with respect to the reference point $A(\cdot)$, the symmetric, positive-definite matrix $\mathfrak{I} \in \mathbb{R}^{3\times 3}$ denotes the *inertia matrix of the aerial robot* with respect to the reference point $A(\cdot)$,

$$f_{\text{dyn, tran}}(t,q,\dot{q}) \triangleq F_g^{\mathbb{I}} - mR(q)\omega^{\times}(q,\dot{q})\omega^{\times}(q,\dot{q})r_C, \tag{43}$$

$$\begin{aligned} f_{\text{dyn, rot}}(t,q,\dot{q}) \triangleq & -\omega^{\times}(q,\dot{q})\mathfrak{I}\omega(q,\dot{q}) \\ & -\sum_{i=1}^{4}\left[\mathfrak{I}_{P_i}(t)\dot{\omega}_{P_i}(t) + \omega_{P_i}^{\times}(t)\mathfrak{I}_{P_i}(t)\omega_{P_i}(t)\right] \\ & -\omega^{\times}(q,\dot{q})\sum_{i=1}^{4}\mathfrak{I}_{P_i}(t)\omega_{P_i}(t) + r_C^{\times}R^{\mathrm{T}}(q)F_g^{\mathbb{I}}, \end{aligned} \tag{44}$$

$$G(q) \triangleq \begin{bmatrix} R(q)\begin{bmatrix}\mathbf{e}_{1,3} & \mathbf{e}_{3,3}\end{bmatrix} & 0_{3\times 3} \\ 0_{3\times 2} & I_3 \end{bmatrix}, \tag{45}$$

$u \triangleq [u_5, u_1, \ldots, u_4]^{\mathrm{T}} \in \mathbb{R}^5$ denotes the control input, $u_5, u_1 : [t_0, \infty) \to \mathbb{R}$, denote the *components of the forces produced by the propellers along the* $x(\cdot)$ *and* $z(\cdot)$ *axes*, respectively, and $[u_2, u_3, u_4]^{\mathrm{T}} : [t_0, \infty) \to \mathbb{R}^3$ denotes the *moment of the force produced by the propellers*.

The inertia matrix of the ith propeller $\mathfrak{I}_{P_i}(\cdot)$, $i = 1, \ldots, 4$, is a function of time since the propellers' tilt angle may vary [3]. The first component of the control vector $u(\cdot)$ is denoted by $u_5(\cdot)$ for consistency with the notation concerning classical quadcopters, for which $u : [t_0, \infty) \to \mathbb{R}^4$ and $u_5(t) \equiv 0$, $t \geq t_0$; for details, see [32].

If $\sigma(t) = 1$, $t \in \bigcup_{k=0}^{\infty}[\tau_{2k}, \tau_{2k+1})$, then $\mathcal{H}_{\sigma(t)} = I_6$, and Eq. 40 captures the aircraft's free flight dynamics. Alternatively, if $\sigma(t) = 2$, $t \in \bigcup_{j=0}^{\infty}[\tau_{2j+1}, \tau_{2(j+1)})$, then $\mathcal{H}_{\sigma(t)} = \begin{bmatrix} 0_{3\times 3} & 0_{3\times 3} \\ 0_{3\times 3} & \begin{bmatrix} 0 & 0 & 0 \\ 0 & 1 & 0 \\ 0 & 0 & 0 \end{bmatrix} \end{bmatrix}$, and Eq. 40 captures the pitch dynamics of the aerial robot while connected to the vertical surface. An equivalent formulation of the aerial robot's dynamics may have been deduced by setting $\mathcal{H}_{\sigma(t)} = I_6$, $t \geq t_0$, and introducing the impulsive reaction forces and moments imposed by the vertical surface in the aerial robot's free flight dynamic equations.

5.3 Control Strategy

Let $q_{\text{ref}}(t) \triangleq \left[\left(r_{\text{ref}}^{\mathbb{I}}(t)\right)^{\mathrm{T}}, \phi_{\text{ref}}(t), \theta_{\text{ref}}(t), \psi_{\text{ref}}(t)\right]^{\mathrm{T}} \in \mathcal{D}$, $t \geq t_0$, denote the piece-wise twice continuously differentiable *reference vector of independent generalized coordinates*, where $r_{\text{ref}}^{\mathbb{I}}(\cdot)$ captures the user-defined *reference trajectory* for the point $A(\cdot)$, $\phi_{\text{ref}}(\cdot)$ captures the *reference roll angle*, $\theta_{\text{ref}}(\cdot)$ captures the user-defined *reference pitch angle*, and $\psi_{\text{ref}}(\cdot)$ captures the user-defined *reference yaw angle*. We design $q_{\text{ref}}(\cdot)$ so that $r_{\text{ref}}^{\mathbb{I}}(t) = r_{\text{wall}}^{\mathbb{I}}$, $t \in \bigcup_{j=0}^{\infty}[\tau_{2j+1}, \tau_{2(j+1)})$, where $r_{\text{wall}}^{\mathbb{I}}$ denotes the point on the vertical surface where the camera must be installed. Furthermore, we set $\theta_{\text{ref}}(t) \equiv 0$, $t \geq t_0$, and $\psi_{\text{ref}}(t) \equiv 0$ so that the robotic arm is orthogonal to the vertical surface upon impact. The aerial robot considered in this research is underactuated since it is characterized by six degrees of freedom, namely the components of $q(\cdot)$, and five control inputs, namely the components of $u(\cdot)$. Therefore, it is impossible to define $q_{\text{ref}}(\cdot)$ arbitrarily. For these aerial vehicles, $\phi_{\text{ref}}(\cdot)$ is deduced so that the desired displacement of the reference point $A(\cdot)$ along the direction Y of the reference frame $\mathbb{I}$ can be achieved [3]. In this paper, we set $\mathbf{e}_{2,3}^{\mathrm{T}} r_{\text{ref}}^{\mathbb{I}}(t) = 0$, $t \geq t_0$, so that if $\left|\mathbf{e}_{2,3}^{\mathrm{T}}\left(r_A^{\mathbb{I}}(t) - r_{\text{ref}}^{\mathbb{I}}(t)\right)\right| = 0$, $t \geq t_0$, then $\phi_{\text{ref}}(t) = 0$.

Next, consider the feedback-linearizing control law

$$\begin{aligned} & \beta_s(t,q,q_{\text{ref}},w) \\ & \triangleq h\Bigg(-\begin{bmatrix} f_{\text{dyn, tran}}(t,q,\dot{q}) \\ f_{\text{dyn, rot}}(t,q,\dot{q}) \end{bmatrix} + \mathcal{M}(q)\begin{bmatrix} \mathbf{1}_3 0_{3\times 3} \\ 0_{3\times 3}\Gamma^{-1}(q) \end{bmatrix} \\ & \cdot\left[\ddot{q}_{\text{ref}} - \begin{bmatrix} 0_{3\times 1} \\ \dot{\Gamma}(q)\omega(q,\dot{q}) \end{bmatrix} - [K_{\mathrm{P},s}, K_{\mathrm{D},s}]\begin{bmatrix} q - q_{\text{ref}} \\ \dot{q} - \dot{q}_{\text{ref}} \end{bmatrix} + w\right]\Bigg), \\ & (s,t,q,q_{\text{ref}},w) \in \Sigma \times [t_0,\infty) \times \mathcal{D} \times \mathcal{D} \times \mathbb{R}^6, \end{aligned} \tag{46}$$

where $K_{\mathrm{P},s}, K_{\mathrm{D},s} \in \mathbb{R}^6$ are user-defined, symmetric, and positive-definite gain matrices that define a proportional-derivative baseline controller, $h : \mathbb{R}^n \to \mathbb{R}^n$ is defined so that $\mathbf{e}_{j,6}^{\mathrm{T}} h(x) = x_j$, $j \in \{1,2,4,5,6\}$, and $\mathbf{e}_{3,6}^{\mathrm{T}} h(x) = \mu_\kappa(x_3)$, and $\mu_\kappa : \mathbb{R} \to \mathbb{R}$ is defined so that $\mu_\kappa(\alpha) = \kappa\,\mathrm{sign}\alpha$, for $|\alpha| \leq \kappa$ and $\kappa > 0$ user-defined and arbitrarily small, and $\mu_\kappa(\alpha) = \alpha$, for $|\alpha| > \kappa$. If $u(t) = \beta_{\sigma(t)}(t, q(t), q_{\text{ref}}(t), w(t))$, $t \geq t_0$, then the trajectory tracking error dynamics is given by the switched dynamical model

$$\begin{aligned} \dot{e}(t) &= A_{\text{ref},\sigma(t)}e(t) + B\left[w(t) + \tilde{\Theta}^{\mathrm{T}}\tilde{\Phi}_{\sigma(t)}(t,q(t),\dot{q}(t))\right], \\ e(t_0) &= \begin{bmatrix} q(t_0) - q_{\text{ref}}(t_0) \\ \dot{q}(t_0) - \dot{q}_{\text{ref}}(t_0) \end{bmatrix}, \qquad t \geq t_0, \end{aligned} \tag{47}$$

where $e(t) \triangleq q(t) - q_{\text{ref}}(t)$, denotes the *trajectory tracking error*, $A_{\text{ref},s} = \begin{bmatrix} 0_{6\times 6} & I_6 \\ -K_{\mathrm{P},s} & -K_{\mathrm{D},s} \end{bmatrix}$, $s \in \Sigma$, $B = \begin{bmatrix} 0_{6\times 6} \\ I_6 \end{bmatrix}$, $\tilde{\Theta} \in \mathbb{R}^{39\times 6}$ is unknown, and

$$\begin{aligned} \tilde{\Phi}_s(t,q,\dot{q}) &\triangleq \left[\mathbf{1}_{\{s\in\Sigma: s-1=0\}}(s)\overline{\Phi}_1^{\mathrm{T}}(t,q,\dot{q}), \mathbf{1}_{\{s\in\Sigma: s-2=0\}}(s)\overline{\Phi}_2(t,q,\dot{q}),\right]^{\mathrm{T}}, \\ & (s,t,q,\dot{q}) \in \Sigma \times [t_0,\infty) \times \mathcal{D} \times \mathbb{R}^6, \end{aligned} \tag{48}$$

$$\begin{aligned} \overline{\Phi}_1(t,q,\dot{q}) &= \Big[-mW_M^{\mathrm{T}}(R(q)\omega^{\times}(q,\dot{q})\omega^{\times}(q,\dot{q})), \\ & \quad -W_M^{\mathrm{T}}\left(\omega^{\times}(q,\dot{q})M_W(\omega(q,\dot{q}))\right), F_g^{\mathrm{T}}(q)\Big]^{\mathrm{T}}, \end{aligned} \tag{49}$$

$$\overline{\Phi}_2(t,q,\dot{q}) = \mathbf{e}_{3,3}^{\mathrm{T}} F_g(q), \tag{50}$$

$$W_M(A) \triangleq \sum_{i=1}^{n}[\mathbf{e}_{i,m} \otimes (A\mathbf{e}_{i,m})], \qquad A \in \mathbb{R}^{n\times m}, \tag{51}$$

$$M_W(b,n) \triangleq \left(b^{\mathrm{T}} \otimes I_n\right), \qquad (b,n) \in \mathbb{R}^m \times \mathbb{N}, \qquad b \in \mathbb{R}^n. \tag{52}$$

The regressor vector $\tilde{\Phi}_s(t, q, \dot{q})$, $(s, t, q, \dot{q}) \in \Sigma \times [t_0, \infty) \times \mathcal{D} \times \mathbb{R}^6$, has been constructed to capture the effect of uncertainties on the location of the aerial robot's center of mass on the right-hand side of the dynamic (40). The function $h(\cdot)$ in Eq. 46 guarantees the controllability of the closed-loop plant dynamics at all times [3].

Let $w(t) = \phi(\hat{\Theta}(t), \tilde{\Phi}_{\sigma(t)}(t, q(t), \dot{q}(t)))$, $t \geq t_0$, where the feedback control law $\phi(\cdot, \cdot)$ is given by Eq. 25 and $\hat{\Theta}(\cdot)$ verifies the adaptive law (21). In this case, the trajectory tracking error dynamics (47) is in the same form as Eq. 20 with $n = 12$, $m = 6$, $x = \left[q^{\mathrm{T}}, \dot{q}^{\mathrm{T}}\right]^{\mathrm{T}}$, and $B_s = B$, $s \in \Sigma$. Therefore, it follows from Theorem 3 or, alternatively, from Theorem 4 that the proposed model reference adaptive control law (25) and the proposed adaptive law (21) can be employed to guarantee satisfactory trajectory tracking at all times.

5.4 Flight Tests Setup

The aerial robot employed to test the proposed model reference adaptive control framework for switched dynamical systems is custom designed. The chassis is made of carbon fiber rods and the propellers are actuated by Dynamixel AX-18A servo motors, which guarantee ± 1 deg precision and allow to measure their displacement. To guarantee successful grasping and placement of the camera sensor and allow the user to release the camera at a desired time instant, a gripper based on an active, self-sealing suction cup has been employed.

The proposed control law has been coded in the C++ programming language and implemented on an ODroid XU4 companion computer, which integrates both (21) and (20) and evaluates the control law (25) at a frequency of approximately 250 Hz. Once the control input $u(\cdot)$ has been determined, the companion computer calculates the tilt angle and thrust force for each propeller to realize the desired control input according to the algorithm outlined in [3]. The servo actuators that regulate the propellers' tilt angles are controlled directly by the companion computer. Each propeller's desired thrust force is transmitted from the companion computer to a Pixhawk 2 flight controller over a dedicated serial line, and the flight controller coordinates each propeller so that the desired thrust force is realized. The flight controller also embeds an inertial measurement unit and an extended Kalman filter to estimate the vehicle's rotational position and velocities. Flight tests have been performed indoors, and the aerial robot's position and velocity are deduced by a Vicon motion capture system and transmitted over WiFi to the companion computer.

5.5 Flight tests results

The feedback-linearizing control law (46) and the adaptive law (21) have been coded assuming that the aerial robot's mass is $m = 2.06$kg, which has been deduced using a precision scale, and its inertia matrix is

$$\mathfrak{I} = \begin{bmatrix} 1.97 & -0.0732 & -0.0182 \\ -0.0732 & 1.37 & -0.0162 \\ -0.0182 & -0.0162 & 10.8 \end{bmatrix} \cdot 10^{-3} kg \cdot m^2,$$

which has been deduced using a computer aided design (CAD) model. Furthermore, the ith propeller's inertia matrix $\mathfrak{I}_{P_i}(\cdot)$, $i = 1, \ldots, 4$, has been computed by modeling each propeller as a thin disk of mass 0.0039 kg and radius 0.1145 m. Lastly, we set $K_{\mathrm{P},1} = \mathrm{diag}(1, 1, 2, 0.4, 0.5, 0.4)$,

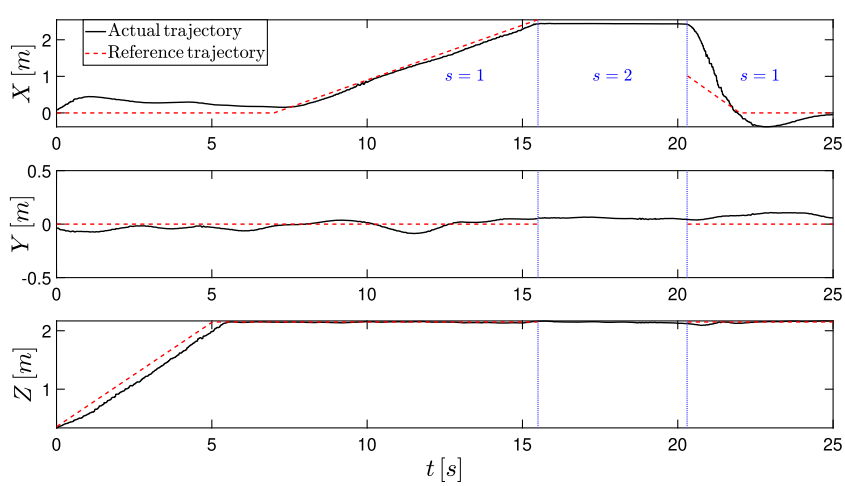

Fig. 7 Position of the aerial robot during a sensor placement mission. Both the feedback-linearizing control law (46) and the adaptive law (21) have been tuned without accounting for the camera. Therefore, during the adaptive gains' transient dynamics over the time interval [0, 7.2] s, the trajectory tracking error is sensibly larger than over the time interval [7.2, 20.3] s. To lead the aerial robot away from the vertical surface as soon as possible and overcome the force exerted by the suction cup, the reference trajectory is discontinuous at $t = 20.3$ s

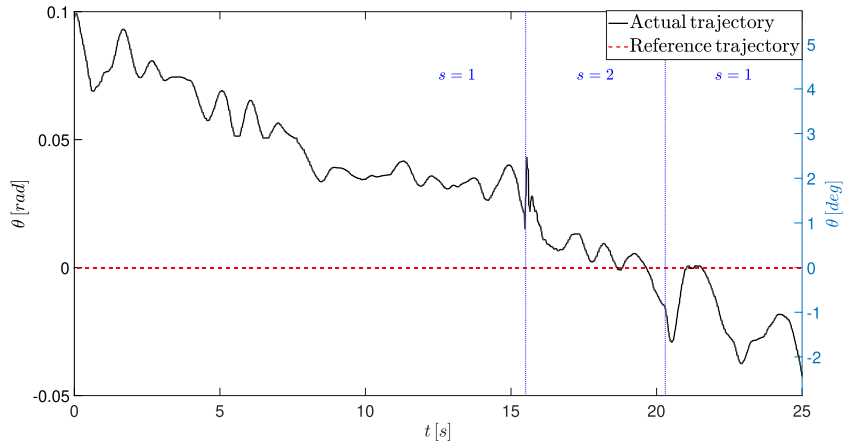

Fig. 8 Pitch angle of the aerial robot. The proportional-derivative baseline controller has been tuned without accounting for the camera. Therefore, the aerial robot experiences a pitch moment due to the gravitational force, which is counteracted by the adaptive control law

$K_{\mathrm{D},1} = \mathrm{diag}(0.5, 0.5, 1, 0.1, 0.25, 0.1)$, $K_{\mathrm{P},2} = 0.5 I_6$, and $K_{\mathrm{D},2} = 0.25 I_6$; the adaptive rate matrix Γ and the matrices P and Q that verify the Lyapunov inequality (26) have been omitted for brevity. The inertial parameters of the camera have been neglected while tuning the proposed controller.

Figure 7 shows the components of both the actual trajectory $r_A^{\mathbb{I}}(\cdot)$ and the reference trajectory $r_{\mathrm{ref}}^{\mathbb{I}}(\cdot)$ of the point $A(\cdot)$. The aircraft takes off at $t = 0$ s and is commanded to reach an altitude of 2.15 m over the time interval $[0, 5]$ s. Successively, the reference trajectory requires the aerial robot to hover for two seconds. At $t = 7$ s, the reference trajectory leads the reference point $A(\cdot)$ toward the wall at a forward velocity of 0.33 m/s. The wall is impacted at $t = 15.5$ s and the propellers' tilt angles are held constant over the time interval $[15.5, 20.3]$ s to exert sufficient horizontal force to engage the fabric strip fastener. At $t = 20.3$ s, the suction cup's micro-pump is deactivated and the aerial robot follows its reference trajectory moving away from the vertical surface. The reference trajectory is discontinuous at $t = 20.3$ s to lead the aerial robot away from the vertical surface as soon as possible and overcome the residual force exerted by the suction cup. Therefore, in this flight test $t_0 = \tau_0 = 0$ s, $\tau_1 = 15.5$ s, and $\tau_2 = 20.3$ s. Although t_0 and τ_2 have been set *a priori*, τ_1 could be only estimated over the course of the flight test, which provided an additional challenge for the proposed control architecture.

Over the time interval $[0, 15.5)$ s, the $\mathcal{L}_\infty$-norm and the $\mathcal{L}_2$-norm of the trajectory tracking error are 0.4820 m and 0.1904 m/s, respectively. Over the time interval $[15.5, 20.3)$ m, the $\mathcal{L}_\infty$-norm and the $\mathcal{L}_2$-norm of the trajectory tracking error are 0.0412 m and 0.0226 m/s, respectively. Finally, over the time interval $[20.3, 25]$ s, the $\mathcal{L}_\infty$-norm and the $\mathcal{L}_2$-norm of the trajectory tracking error are 1.4270 m and 0.4054 m/s, respectively. The target position $r_{\mathrm{wall}}^{\mathbb{I}} = [2.15, 0, 2.15]^{\mathrm{T}}$ m is reached with 0.01 m error at $t = \tau_1$. The proposed control architecture has been tuned without accounting for the camera, which lead to larger initial errors in the trajectory tracking error along both the X axis and the Z axis, which are compensated over the time interval $[0, 7.2]$ s. The discontinuity in the reference trajectory $q_{\mathrm{ref}}(\cdot)$ lead to a large trajectory tracking error, which is compensated over the time interval $[20.3, 25]$ s.

Figure 8 shows the aerial robot's pitch angle. Over the time interval $[0, 15.5)$ s, the $\mathcal{L}_\infty$-norm and the $\mathcal{L}_2$-norm of the pitch tracking error are 0.0993 and 0.1042 s^{-1}, respectively. Over the time interval $[15.5, 20.3)$ s, the $\mathcal{L}_\infty$-norm and the $\mathcal{L}_2$-norm of the pitch tracking error are 0.0430 and 0.0177 s^{-1}, respectively. Finally, over the time interval $[20.3, 25]$ s, the $\mathcal{L}_\infty$-norm and the $\mathcal{L}_2$-norm of the pitch tracking error are 0.0423 and 0.0398 s^{-1}, respectively. Since the proposed control architecture has been tuned without accounting for the payload, the aerial robot experiences a positive pitch angle over the time interval $[0, 15.5]$ s. The reaction force produced by disengaging the suction cup from the wall produced a negative moment and hence, a negative pitch angle over the time interval $[20.3, 25]$ s.

6 Conclusion

This paper presented a model reference adaptive control framework for unknown nonlinear switched plants, whose trajectory of a user-defined linear switched reference model. For the first time, the effectiveness of a model reference adaptive control law for unknown nonlinear switched plants is proven by analyzing both Carathéodory and Filippov solutions. The effectiveness of the proposed results have been verified both numerically and by means of flight tests. The proposed numerical simulation involves the design of an adaptive control law for a reconfigurable delta-wing aircraft, whose aerodynamic and geometric coefficients vary instantly and are unknown. The proposed flight tests involve the design of a control law for an aerial robot tasked with installing a camera of unknown inertial properties at a user-defined point on a vertical surface.

References

1. Alexis, K., Darivianakis, G., Burri, M., Siegwart, R.: Aerial robotic contact-based inspection: Planning and control. Auton. Robot. **40**(4), 631–655 (2016). https://doi.org/10.1007/s10514-015-9485-5
2. Anderson, R.B.: Flight experiment of a tilt-rotor quadcopter installing a camera. https://youtu.be/f6wG7IdPXoc. Last accessed 11/29/2019 (2019)
3. Anderson, R.B., Burke, J.P., Marshall, J.A., L'Afflitto, A.: Robust Adaptive Control for Constrained Tilt-Rotor Quadcopters of Unknown Inertial Properties. In: American Control Conference, pp. 2922–2927. https://doi.org/10.23919/ACC.2019.8814780 (2019)
4. Ang, K.Z.Y., Cui, J., Pang, T., Li, K., Wang, K., Ke, Y., Chen, B.M.: Development of an Unmanned Tail-Sitter with Reconfigurable Wings: U-Lion. In: IEEE International Conference on Control Automation, pp. 750–755. https://doi.org/10.1109/ICCA.2014.6871015 (2014)
5. Bardi, M., Capuzzo-Dolcetta, I.: Optimal Control and Viscosity Solutions of Hamilton-Jacobi-Bellman Equations. Birkhäuser, Boston (2008)
6. Brogliato, B.: Nonsmooth Mechanics: Models, Dynamics and Control. Communications and Control Engineering. Springer, London (1999)
7. Bryson, A.E.: Applied Optimal Control: Optimization, Estimation and Control. Taylor & Francis, New York (1975)
8. Carathéodory, C.: Vorlesungen Über Reelle Funktionen. Teubner, Berlin (1918)
9. Cheng, H., Dong, C., Jiang, W., Wang, Q., Hou, Y.: Nonfragile switched h_∞ control for morphing aircraft with asynchronous switching. Chin. J. Aeronaut. **30**(3), 1127–1139 (2017). https://doi.org/10.1016/j.cja.2017.01.008
10. Chiang, M.L., Fu, L.C.: Adaptive stabilization of a class of uncertain switched nonlinear systems with backstepping control. Automatica **50**(8), 2128–2135 (2014)
11. Clarke, F.H.: Optimization and nonsmooth analysis. Society of Industrial and Applied Mathematics, Philadelphia (1989)
12. Clarke, F.H., Ledyaev, Y.S., Stern, R.J., Wolenski, P.R.: Nonsmooth analysis and control theory. Graduate texts in mathematics. springer, New York NY (1997)
13. Cortés, J.: Discontinuous dynamical systems. IEEE Control. Syst. Mag. **28**(3), 36–73 (2008). https://doi.org/10.1109/MCS.2008.919306
14. Edwards, C., Spurgeon, S.: Sliding Mode Control: Theory And Applications. Series in Systems and Control. Taylor & Francis, New York (1998)
15. Federer, H.: Geometric measure theory. Springer, Berlin (2014)
16. Filippov, A.F.: Differential Equations with Discontinuous Right-hand Sides. Springer, Amesterdam (1988)
17. Fischer, N., Kamalapurkar, R., Dixon, W.E.: LaSalle-Yoshizawa corollaries for nonsmooth systems. IEEE Trans. Autom. Control **58**(9), 2333–2338 (2013). https://doi.org/10.1109/TAC.2013.2246900
18. Gong, L., Wang, Q., Dong, C.: Disturbance rejection control of morphing aircraft based on switched nonlinear systems. Nonlinear Dyn. **96**(2), 975–995 (2019). https://doi.org/10.1007/s11071-019-04834-9
19. Haddad, W.M., Chellaboina, V.: Nonlinear Dynamical Systems and Control: A Lyapunov-based Approach. Princeton University Press, Princeton (2008)
20. Hájek, O.: Discontinuous differential equations, i. J. Differ. Equ. **32**(2), 149–170 (1979). https://doi.org/10.1016/0022-0396(79)90056-1
21. Heredia, G., Duran, A., Ollero, A.: Modeling and simulation of the HADA reconfigurable UAV. J. Intell. Robot. Syst. **65**(1), 115–122 (2012). https://doi.org/10.1007/s10846-011-9561-9
22. Hespanha, J.P., Liberzon, D., Morse, A.S.: Overcoming the limitations of adaptive control by means of logic-based switching. Syst. Control Lett. **49**(1), 49–65 (2003). https://doi.org/10.1016/S0167-6911(02)00342-0
23. Hu, S.: Differential equations with discontinuous right-hand sides. J. Math. Anal. Appl **154**(2), 377–390 (1991). https://doi.org/10.1016/0022-247X(91)90044-Z
24. Jiang, H.B.: Hybrid adaptive and impulsive synchronisation of uncertain complex dynamical networks by the generalised Barbalat's lemma. IET Control Theory Appl. **3**(10), 1330–1340 (2009). https://doi.org/10.1049/iet-cta.2008.0335
25. Jiao, X., Jiang, J.: Design of adaptive switching control for hypersonic aircraft. Adv. Mech. Eng. **7**(10), 1687814015610, 465 (2015). https://doi.org/10.1177/1687814015610465
26. Kamalapurkar, R., Rosenfeld, J.A., Parikh, A., Teel, A.R., Dixon, W.E.: Invariance-like results for nonautonomous switched systems. IEEE Trans. Autom. Control **64**(2), 614–627 (2019). https://doi.org/10.1109/TAC.2018.2838055
27. Khalil, H.K.: Nonlinear systems. Prentice Hall, Princeton (2002)
28. Kosmatopoulos, E.B., Ioannou, P.A.: A switching adaptive controller for feedback linearizable systems. IEEE Trans. Autom. Control **44**(4), 742–750 (1999). https://doi.org/10.1109/9.754811
29. Koutsoukos, X.D., Antsaklis, P.J., Stiver, J.A., Lemmon, M.D.: Supervisory control of hybrid systems. Proc. IEEE **88**(7), 1026–1049 (2000). https://doi.org/10.1109/5.871307
30. Krasovskii, N.N.: Stability of Motion. Applications of Lyapunov's Second Method to Differential Systems and Equations With Delay. Stanford University Press, Stanford (1963)
31. L'Afflitto, A.: A mathematical perspective on flight dynamics and control. Springer, London (2017)
32. L'Afflitto, A., Anderson, R.B., Mohammadi, K.: An introduction to nonlinear robust control for unmanned quadrotor aircraft: How to design control algorithms for quadrotors using sliding mode control and adaptive control techniques. IEEE Control. Syst. Mag. **38**(3), 102–121 (2018). https://doi.org/10.1109/MCS.2018.2810559
33. Lavretsky, E., Wise, K.: Robust and adaptive control: With aerospace Spplications. springer, London (2012)
34. Levant, A.: Introduction to High-Order Sliding Modes. In: Perruquetti, W., Barbot, J.P. (eds.) Sliding Mode Control in Engineering, Chapter 1. Marcel Dekker, Inc., Basel (2002)
35. Li, Y., Sui, S., Tong, S.: Adaptive fuzzy control design for stochastic nonlinear switched systems with arbitrary switchings and unmodeled dynamics. IEEE Trans. Cybern. **47**(2), 403–414 (2016)
36. Liberzon, D.: Switching in systems and control. Springer, Boston (2003)
37. Marconi, L., Naldi, R.: Control of aerial robots: Hybrid force and position feedback for a ducted fan. IEEE Control. Syst. Mag. **32**(4), 43–65 (2012). https://doi.org/10.1109/MCS.2012.2194841
38. Marconi, L., Naldi, R., Gentili, L.: Modelling and control of a flying robot interacting with the environment. Automatica **47**(12), 2571–2583 (2011). https://doi.org/10.1016/j.automatica.2011.09.020
39. Miller, D.E., Davison, E.J.: An adaptive controller which provides an arbitrarily good transient and steady-state response. IEEE Trans. Autom. Control **36**(1), 68–81 (1991). https://doi.org/10.1109/9.62269
40. Minyue, F., Barmish, B.: Adaptive stabilization of linear systems via switching control. IEEE Trans. Autom. Control **31**(12), 1097–1103 (1986). https://doi.org/10.1109/TAC.1986.1104187

41. Morse, A.S.: Supervisory control of families of linear set-point controllers – Part 1: Exact matching. IEEE Trans. Autom. Control **41**(10), 1413–1431 (1996). https://doi.org/10.1109/9.539424
42. Morse, A.S.: Supervisory control of families of linear set-point controllers – Part 2: Robustness. IEEE Trans. Autom. Control **42**(11), 1500–1515 (1997). https://doi.org/10.1109/9.649687
43. Narendra, K.S., Balakrishnan, J.: Adaptive control using multiple models. IEEE Trans. Autom. Control **42**(2), 171–187 (1997). https://doi.org/10.1109/9.554398
44. Paden, B., Sastry, S.: A calculus for computing Filippov's differential inclusion with application to the variable structure control of robot manipulators. IEEE Trans. Circ. Syst. **34**(1), 73–82 (1987). https://doi.org/10.1109/TCS.1987.1086038
45. Pfeiffer, F., Glocker, C.: Multibody Dynamics with Unilateral Contacts. Springer, Vienna (2000)
46. Seigler, T.M., Neal, D.A., Bae, J.S., Inman, D.J.: Modeling and flight control of large-scale morphing aircraft. AIAA J. Aircraft **44**(4), 1077–1087 (2007). https://doi.org/10.2514/1.21439
47. Shorten, R.N., Narendra, K.S.: On common quadratic Lyapunov functions for pairs of stable LTI systems whose system matrices are in companion form. IEEE Trans. Autom. Control **48**(4), 618–621 (2003). https://doi.org/10.1109/TAC.2003.809795
48. Sofla, A., Meguid, S., Tan, K., Yeo, W.: Shape morphing of aircraft wing: Status and challenges. Mater. Des. **31**(3), 1284–1292. https://doi.org/10.1016/j.matdes.2009.09.011 (2010)
49. Spraker, J.S., Biles, D.C.: A comparison of the Carathéodory and Filippov solution sets. J. Math. Anal. Appl. **198**(2), 571–580 (1996). https://doi.org/10.1006/jmaa.1996.0099
50. Stein, E.M., Shakarchi, R.: Real analysis. Princeton, Princeton (2009)
51. Tan, C., Tao, G., Qi, R., Yang, H.: A direct MRAC based multivariable multiple-model switching control scheme. Automatica **84**, 190–198 (2017). https://doi.org/10.1016/j.automatica.2017.07.020
52. Utkin, V.I.: Sliding Mode Control: Mathematical Tools, Design and Applications, pp. 289–347. Springer, Berlin. https://doi.org/10.1007/978-3-540-77653-6_5 (2008)
53. Vasista, S., Tong, L., Wong, K.: Realization of morphing wings: A multidisciplinary challenge. AIAA J. Aircraft **49**(1), 11–28 (2012). https://doi.org/10.2514/1.C031060
54. Vu, L., Liberzon, D.: Supervisory control of uncertain linear time-varying systems. IEEE Trans. Autom. Control **56**(1), 27–42 (2011). https://doi.org/10.1109/TAC.2010.2060244
55. Wang, Q., Hou, Y., Dong, C.: Model reference robust adaptive control for a class of uncertain switched linear systems. Int. J. Robust Nonlinear Control **22**(9), 1019–1035 (2012). https://doi.org/10.1002/rnc.1744
56. Wang, X., Zhao, J., Tang, Y.: State tracking model reference adaptive control for switched nonlinear systems with linear uncertain parameters. J. Control Theory Appl. **10**(3), 354–358 (2012). https://doi.org/10.1007/s11768-012-1018-6
57. Wu, C., Zhao, J., Sun, X.M.: Adaptive tracking control for uncertain switched systems under asynchronous switching. Int. J. Robust Nonlinear Control **25**(17), 3457–3477 (2015). https://doi.org/10.1002/rnc.3275
58. Xie, J., Li, S., Yan, H., Yang, D.: Model reference adaptive control for switched linear systems using switched multiple models control strategy. J. Frankl. Inst. **356**(5), 2645–2667 (2019). https://doi.org/10.1016/j.jfranklin.2018.10.036
59. Xie, J., Zhao, J.: Model reference adaptive control for switched LPV systems and its application. IET Control Theory Appl. **10**(17), 2204–2212 (2016). https://doi.org/10.1049/iet-cta.2015.1332
60. Xie, J., Zhao, J.: Model reference adaptive control for nonlinear switched systems under asynchronous switching. Int. J. Adapt. Control Signal Process. **31**(1), 3–22 (2017). https://doi.org/10.1002/acs.2666
61. Xie, J., Zhao, J.: h_∞ model reference adaptive control for switched systems based on the switched closed-loop reference model. Nonlinear Anal. Hybrid Syst. **27**, 92–106 (2018). https://doi.org/10.1016/j.nahs.2017.07.003
62. Xie, W., Wen, C., Li, Z.: Input-to-state stabilization of switched nonlinear systems. IEEE Trans. Autom. Control **46**(7), 1111–1116 (2001). https://doi.org/10.1109/9.935066

Robert B. Anderson received the B.S. in Engineering Physics (2017) and the M.S. in Aerospace Engineering (2019) from the University of Oklahoma. Since 2016, he has been a part of the Advanced Control Systems Lab under Dr. L'Afflitto's advisement. His research interests include nonlinear robust control and integrated guidance and control systems with applications to autonomous robots and UAVs. Mr. Anderson was recognized as one of the top 8 undergraduate student interns at the Army Research Lab in the summer of 2017, and is currently pursuing a Ph.D. in Industrial and Systems Engineering at Virginia Tech.

Julius A. Marshall received the B.S. degree in Aerospace Engineering from the University of Oklahoma in 2018. Since 2018, he has been a part of the Advanced Control Systems Lab under Dr. L'Afflitto's advisement. Mr. Marshall is pursuing a Ph.D. degree in Industrial and Systems Engineering at Virginia Tech, where he is specializing in robotics. His current research interests include robust control, optimal control, guidance and navigation, and adaptive control for autonomous shipboard landing. In 2019, he received the SMART Scholar award.

Andrea L'Afflitto received the B.S. degree in Aerospace Engineering and the M.S. degree in Aerospace Engineering and Astronautics from the University of Napoli "Federico II," Italy, in 2004 and 2006, respectively, the M.S. degree in Mathematics from Virginia Tech in 2010, and the Ph.D. in Aerospace Engineering from Georgia Tech in 2015. In 2019, he joined the Grado Department of Industrial and Systems Engineering at Virginia Tech as an assistant professor, from 2015 to 2019, he worked at the School of Aerospace and Mechanical Engineering of the University of Oklahoma as an assistant professor, and from 2008 to 2009 he worked as System Engineer at the German Aerospace Agency (DRL) in Cologne, Germany. Dr. L'Afflitto's current research interests include nonlinear robust control, optimal control, and control of unmanned aerial systems. In 2018, he received the DARPA Young Faculty Award. Dr. L'Afflitto is a member of the IEEE Aerospace Controls Technical Committee.

James M. Dotterweich is a robotics research engineer with the Combat Capabilities Development Command Army Research Laboratory (CCDC ARL) in Aberdeen Maryland, USA. He received his Master of Science in Mechanical Engineering with a robotics focus from The University of Utah, Salt Lake City, UT, USA in 2015. He received his Bachelor's degree in Aerospace Engineering from The University of Colorado at Boulder, CO, USA in 2008. He has been working on robotic systems and software development for unmanned aerial and ground vehicles for ARL for the past six years.